The Plant Cell, Vol. 21: 2811–2828, September 2009, www.plantcell.org

Medicago N_2-Fixing Symbiosomes Acquire the Endocytic Identity Marker Rab7 but Delay the Acquisition of Vacuolar Identity [W]

Erik Limpens,[a] Sergey Ivanov,[a,b] Wilma van Esse,[a] Guido Voets,[a] Elena Fedorova,[a,b] and Ton Bisseling[a,1]

[a] Laboratory of Molecular Biology, Graduate School of Experimental Plant Sciences, Wageningen University, 6708 PB Wageningen, The Netherlands

[b] K.A. Timiryazev Institute of Plant Physiology, Russian Academy of Sciences, Moscow 127392, Russia

Rhizobium **bacteria form N_2-fixing organelles, called symbiosomes, inside the cells of legume root nodules. The bacteria are generally thought to enter the cells via an endocytosis-like process. To examine this, we studied the identity of symbiosomes in relation to the endocytic pathway. We show that in *Medicago truncatula*, the small GTPases Rab5 and Rab7 are endosomal membrane identity markers, marking different (partly overlapping) endosome populations. Although symbiosome formation is considered to be an endocytosis-like process, symbiosomes do not acquire Rab5 at any stage during their development, nor do they accept the trans-Golgi network identity marker SYP4, presumed to mark early endosomes in plants. By contrast, the endosomal marker Rab7 does occur on symbiosomes from an early stage of development when they have stopped dividing up to the senescence stage. However, the symbiosomes do not acquire vacuolar SNAREs (SYP22 and VTI11) until the onset of their senescence. By contrast, symbiosomes acquire the plasma membrane SNARE SYP132 from the start of symbiosome formation throughout their development. Therefore, symbiosomes appear to be locked in a unique SYP132- and Rab7-positive endosome stage and the delay in acquiring (lytic) vacuolar identity (e.g., vacuolar SNAREs) most likely ensures their survival and maintenance as individual units.**

INTRODUCTION

Legume plants have the unique ability to host N_2-fixing *Rhizobium* bacteria inside cells of a newly formed organ, the so-called root nodule. The bacteria are thought to enter nodule cells through an endocytosis-like process and are maintained as host membrane–bound compartments, called symbiosomes, that each contain one (or a few) bacterium (Roth and Stacey, 1989). By multiplication, ultimately thousands of individual N_2-fixing symbiosomes are present in an infected nodule cell.

Endocytosis is a ubiquitous cellular process involving vesicle-mediated transport of extracellular material from the plasma membrane to a lytic compartment, lysosomes in animal cells, and vacuoles in plants. This transport is performed by distinct membrane structures, so-called early and late endosomes, which are involved in subsequent steps of transport. Upon endocytosis, vesicles are first targeted to early endosomes where material that needs to be degraded is sorted and transported further to late endosomes that finally fuse with lysosomes or the lytic vacuole (Pelham, 2002; Perret et al., 2005; Samaj et al., 2005; Geldner and Jürgens, 2006; Mo et al., 2006; Jaillais et al., 2008; Robinson et al., 2008; Ebine and Ueda, 2009).

[1] Address correspondence to ton.bisseling@wur.nl.
The author responsible for distribution of materials integral to the findings presented in this article in accordance with the policy described in the Instruction for Authors (www.plantcell.org) is: Erik Limpens (erik.limpens@wur.nl).
[W] Online version contains Web-only data.
www.plantcell.org/cgi/doi/10.1105/tpc.108.064410

The endocytic-like entry of rhizobia into nodule cells shows some similarity to phagocytosis of bacteria into animal cells. In general, this process involves a maturation of the plasma membrane–derived bacterium-containing endosome/phagosome to eventually fuse with a lytic compartment (Vieira et al., 2002). This maturation requires a sequential interaction with the different compartments of the endocytic pathway. By analogy, it is therefore of interest to determine whether symbiosomes share properties with compartments of the plant endocytic pathway and if so how targeting to a lytic vacuole is avoided.

The different endosome compartments can be distinguished by the presence of specific membrane identity markers, such as regulatory small GTPases of the Rab family and SNARE (*N*-ethylmaleimide-sensitive factor attachment protein receptor) proteins (Sanderfoot et al., 2000; Pfeffer and Aivazian, 2004; Seabra and Wasmeier, 2004; Behnia and Munro, 2005; Lipka et al., 2007; Pfeffer, 2007; Sanderfoot, 2007; Bassham and Blatt 2008; Nielsen et al., 2008). These proteins control the specificity of membrane fusion events at the compartments where they reside. Rab GTPases control the transport and docking of vesicles after which a vesicle-associated SNARE protein forms a complex with complementary SNARE proteins in the target compartment that drives the fusion. Well-studied identity markers of the endocytic pathway in animals and yeast are the small GTPases Rab5 and Rab7, which control early and late endosome interactions, respectively.

Several bacterial pathogens of animal cells are able to avoid the fusion of their pathogen-containing compartment with lysosomes to ensure their maintenance and multiplication (Alonso and Garcia-del Portillo, 2004). Such intracellular pathogens manipulate the endocytic pathway, with the result that their

membrane compartment does not undergo the normal phagocytic maturation route (Via et al., 1997; Knodler et al., 2001; Brumell and Grinstein, 2004; Behnia and Munro, 2005). By manipulating the association of distinct membrane identity markers, they either stop or segregate from the default phagocytic pathway to the lysosome. For example, *Mycobacterium bovis* vacuoles retain the early endosome marker Rab5 and do not acquire the late endosomal Rab7, thereby preventing the fusion with lysosomes (Via et al., 1997). So they become locked in an early endosome stage. We hypothesized that rhizobia might similarly manipulate the endocytic pathway to maintain symbiosomes and avoid fusion with lytic compartments.

Among the best-studied endosomal proteins in plants are the *Arabidopsis thaliana* Rab5 homologs (Ueda et al., 2001, 2004). *Arabidopsis* contains three Rab5 homologs: Ara7/RabF2b and Rha1/RabF2a, which are most homologous to yeast and animal Rab5s, and Ara6/RabF1, which represents a plant unique Rab5 homolog (Ueda et al., 2001). Ara6/RabF1 and Ara7/Rha1 have been shown to occur in distinct, yet overlapping, endosome populations in *Arabidopsis* (Ueda et al., 2004) that both are characterized as multivesicular bodies (MVBs) (Tse et al., 2004; Haas et al., 2007; Lam et al., 2007). Furthermore, the Rab5-labeled endosomes were also named prevacuolar compartments (PVCs) as they contain vacuolar sorting receptors and interfering with their function affected the proper trafficking of vacuolar proteins from the Golgi to the vacuole (Li et al., 2002; Paris and Neuhaus, 2002; Sohn et al., 2003; Surpin et al., 2003; Bolte et al., 2004; Kotzer et al., 2004; Tse et al., 2004; Foresti et al., 2006; Otegui et al., 2006). This implies that the endocytic pathway and the vacuolar biosynthetic pathway merge at Rab5 PVCs. In plants, Rab5 PVCs are considered to represent late endosome compartments as they are in yeast, whereas in animal cells, Rab5-labeled endosomes are early endosomes (Gerrard et al., 2000; Pelham, 2002; Jürgens, 2004; Surpin and Raikhel, 2004; Samaj et al., 2005; Jaillais et al., 2008). The trans-Golgi network (TGN) is now thought to represent the early endosome compartment in plants, similar to the situation in yeast (Dettmer et al., 2006; Lam et al., 2007a, 2007b; Chow et al., 2008; Robert et al., 2008; Robinson et al., 2008; Ebine and Ueda 2009). However, the exact organization of the plant TGN and the transport steps it is involved in still need to be better defined.

Rab7 GTPase generally is thought to be required for the formation of lytic compartments (Bucci et al., 2000). Animal and yeast cells generally contain a single Rab7 protein, which localizes to late endosomes and to lysosomes/vacuoles (Schimmöller and Riezman, 1993; Bruckert et al., 2000; Bucci et al., 2000; Pelham, 2002). By contrast, *Arabidopsis* contains 8 Rab7 homologs, which suggests that they have several specialized functions possibly related to the multiple vacuole types found in plants (Rutherford and Moore, 2002; Surpin et al., 2003; Sanderfoot, 2007; Sanmartín et al., 2007; Nielsen et al., 2008). Rab7 proteins have been localized to the tonoplast in both *Arabidopsis* and rice (*Oryza sativa*; Saito et al., 2002; Nahm et al., 2003); however, they have not been studied much in plants. Furthermore, Rab7 proteins have been implicated in symbiosome maintenance in soybean (*Glycine max*; Cheon et al., 1993; Son et al., 2003), and several Rab7 homologs were identified in a proteomics study of symbiosomes in *Lotus japonicus* (Wienkoop and Saalbach, 2003). This suggests that symbiosome formation may have hijacked the endocytic pathway to become a vacuole-like compartment (Mellor, 1989).

To test the hypothesis that symbiosomes manipulate the endocytic machinery for their maintenance, we first mainly focused on the key endosomal Rab GTPases, Rab5 and Rab7, during symbiosome development in the model legume *Medicago truncatula*. *Medicago* nodules have a persistent meristem at their apex by which new cells are continuously added to the nodule tissues. Therefore, these tissues are of graded age with the youngest cells adjacent to the meristem and the oldest cells near the root attachment site. The bacteria are continuously released as symbiosomes from cell wall–bound infection threads in two to three cell layers directly adjacent to the meristem. After symbiosomes are taken up into the cells, they start to divide and finally differentiate into their N_2-fixing form. The zone where release and subsequent division and differentiation of symbiosomes occur is called the infection zone. This zone is followed by the fixation zone where symbiosomes are N_2-fixing organelles. In older nodules, senescence is induced in the basal, most proximal to the root part of the nodule (senescence zone). Senescence starts with the fusion and formation of lytic symbiosome compartments (Vasse et al., 1990; Van de Velde et al., 2006). The resulting age gradient provides a strong experimental system to study symbiosome properties at subsequent stages of development in single longitudinal nodule sections.

Here, we show that symbiosomes do not make use of the known/default endocytic pathway in *Medicago* to enter nodule cells. We show that symbiosomes do acquire the endosomal marker Rab7 when they stop diving and that Rab7 specifically regulates the maturation of the symbiosomes into a nitrogen-fixing organelle. Furthermore, symbiosomes seem to be maintained as individual membrane compartments by delaying the acquisition of vacuolar SNAREs.

RESULTS

Identification of *Medicago* Rab5 and Rab7 Homologs

To study the involvement of the endocytic pathway in symbiosome formation, we first identified markers for the endosomal compartments in *Medicago*. We initially focused on the key endosomal small GTPases of the Rab family, Rab5 and Rab7. In *Medicago*, three Rab5 homologs, Rab5A1 (TC106962), Rab5A2 (TC106963), and Rab5B (TC93994), were identified in the available genomic and cDNA sequences. All three *Medicago* Rab5 homologs are represented in nodule cDNA libraries. *Medicago* Rab5A1 and Rab5A2 are most homologous to the two conserved Rab5s of *Arabidopsis*, Ara7/RabF2b and Rha1/RabF2a, whereas *Medicago* Rab5B is most homologous to Rab5 unique for plants (e.g., *Arabidopsis* Ara6/RabF1; see Supplemental Figure 1 online) (Ueda et al., 2001). *Medicago* Rab5A1 and Rab5A2 contain the C-terminal Cys-motif that is highly conserved in most Rab GTPases and represents a site for isoprenylation. By contrast, *Medicago* Rab5B lacks this C-terminal Cys motif, but it contains the N-terminal domain characteristic for Rab5 unique to plants that is most likely acylated (Ueda et al., 2001).

The *Medicago* genome contains at least eight Rab7 homologs (see Supplemental Figure 1 online). Only two Rab7 ESTs, Rab7A1 (TC101145) and Rab7A2 (TC94423), were represented in nodule cDNA libraries; therefore, we focused on these two Rab7 proteins.

The expression of the three *Rab5* and two *Rab7* genes in 10-d-old and 3-week-old nodules was verified using real-time RT-PCR and their expression level appeared largely similar to that in roots (see Supplemental Figure 2 online). Furthermore, microarray analyses on RNA from infected cells isolated by laser capture microdissection showed that all genes that we selected in this study are active in the cells containing symbiosomes (E. Limpens, unpublished data).

Rab5s Occur on Endosomes

To study whether the *Medicago* Rab5 proteins localize to endosomal membrane compartments, we generated transgenic *Medicago* roots that express green fluorescent protein (GFP) fusion constructs via *Agrobacterium rhizogenes*–mediated root transformation. Rab5A1 and RabA2 were fused to the C terminus of GFP, while Rab5B, which is likely N-acylated, was fused to the N terminus of GFP. The GFP Rab5 fusion constructs were expressed under control of the cauliflower mosaic virus *35S* promoter and/or the *Arabidopsis Ubiquitin3* promoter, and the subcellular localization of the fusion proteins was studied by confocal microscopy in the elongation zone (Figure 1) and root hairs.

All three Rab5 fusion proteins localized to small, highly mobile, dot-like structures within the cytoplasm (Figure 1A; see Supplemental Figure 3 online). These small dots are most likely endosomes as described for *Arabidopsis* (Ueda et al., 2001, 2004). In addition, larger structures labeled by Rab5s were observed, most likely representing clusters of endosomes. Although Ara6 and Ara7/Rha1 were shown to label distinct but overlapping endosome populations in *Arabidopsis*,

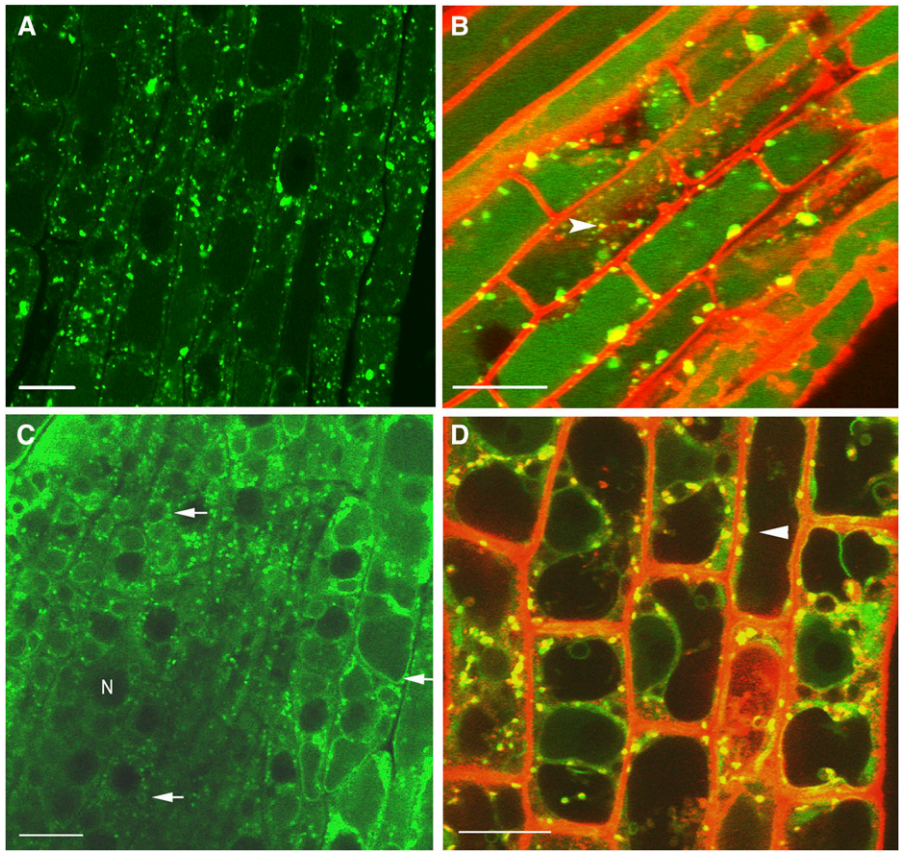

Figure 1. Rab5 and Rab7 Occur on Endosomes.

(A) to **(D)** Confocal image of *p35S:GFP-Rab5A2* (**[A]** and **[B]**) and *p35S:GFP-MtRab7A2* (**[C]** and **[D]**) expressing *Medicago* roots. Bars = 10 μm.
(A) GFP-MtRab5A2 marks dot-like structures. Similar localization patterns were observed for Rab5A1 and Rab5B (see Supplemental Figure 3 online).
(C) GFP-Rab7A2 (as well as GFP-Rab7A1; see Supplemental Figure 3 online) marks dot-like structures as well as the tonoplast of small and large vacuoles (arrows).
(B) and **(D)** Pulse chase (45 min) with the fluorescent endosomal tracer FM4-64. Yellow dots represent the colocalization of GFP and red fluorescent FM4-64 signal, showing that the structures are endosomes. At this time point, FM4-64 does not yet label the tonoplast. N, nucleus; arrow, vacuole; arrowhead, colocalization of red and green signals.

we did not study to what extent the populations marked by the different Rab5s overlap in *Medicago*.

To verify that the Rab5-labeled dots represent compartments of the endocytic pathway, we performed a pulse-chase experiment with the fluorescent endosomal tracer FM4-64. FM4-64 is a lipophylic styryl dye that fluoresces upon insertion into membranes and can only enter cells through endocytic uptake (Ueda et al., 2001, 2004; Tse et al., 2004; Samaj et al., 2005). FM4-64 partly colocalized with GFP-Rab5 (similar for all three Mt Rab5s) before FM4-64 labeling of the tonoplast occurred (Figure 1B; see Supplemental Figure 3 online). This indicates that the Rab5-labeled compartments indeed represent endosomes.

To verify that the GFP-tagged Rab5 proteins are targeted to the same compartments as their endogenous counterparts, we performed immunolocalization studies using an antibody specific for Rab5 (anti-Ara7 from *Arabidopsis*). This showed that in transgenic *GFP-Rab5*–expressing roots, GFP and anti-Rab5 show a very high level of colocalization (Figure 2A). Furthermore, in nontransgenic roots, a similar number of Rab5-containing dot-like structures are observed (recognized by anti-Ara7). So neither the use of heterologous promoters nor the presence of the GFP tag affected proper targeting of Rab5.

To determine the ultrastructural properties of Rab5-labeled compartments, the localization of the Rab5 fusion proteins was analyzed by electron microscopy (EM). EM immunogold labeling with an anti-GFP antibody was used to localize the GFP fusion proteins in the elongation zone of transgenic roots. Rab5 proteins occurred specifically on membrane compartments with a diameter of 100 to 300 nm containing internal membranes (Figures 3A and 3B). So they are structurally similar to MVBs

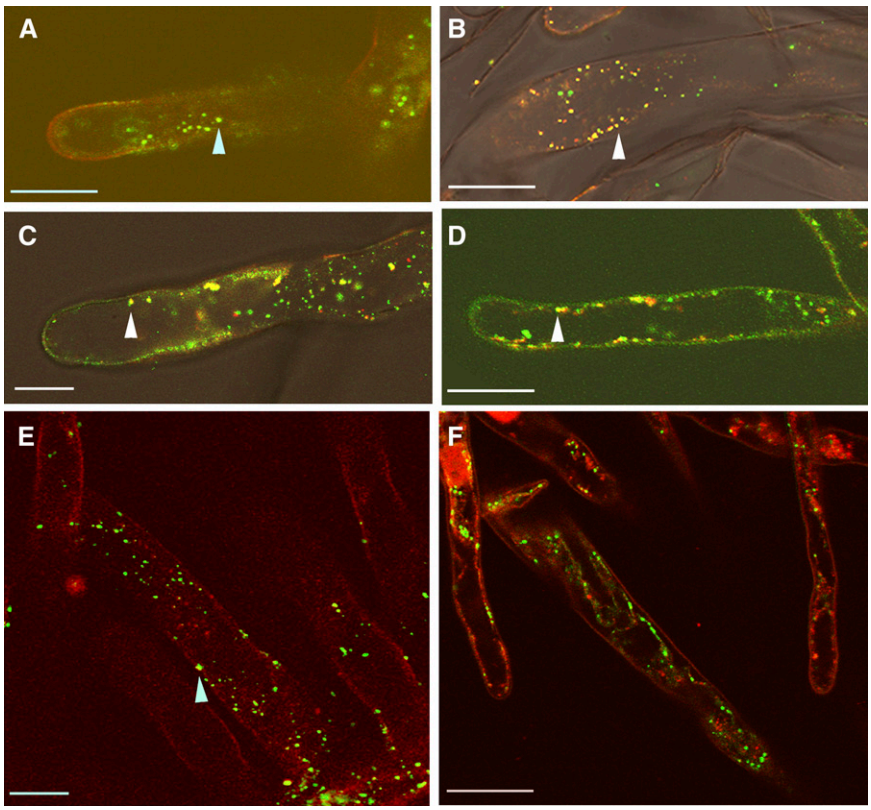

Figure 2. Rab5 Marks Prevacuolar Compartments, While Rab7 Marks Different, Partly Overlapping Endosome Populations.

(A) Immunolocalization of anti-Rab5 (anti-Ara7) (secondary antibody CY3-tagged; red) on *p35S:GFP-Rab5A2*–expressing root hairs, showing a high level of colocalization (yellow signal; arrow).

(B) Immunolocalization of anti-BP-80 (secondary antibody CY3-tagged; red) on *p35S:GFP-Rab5B*–expressing root hairs.

(C) Immunolocalization of anti-BP-80 (red) on *p35S:GFP-Rab5A2*–expressing root hairs. The high level of colocalization (yellow signal; arrow) in **(B)** and **(C)** indicates that the Rab5-labeled endosomes represent PVC compartments.

(D) Immunolocalization of anti-Rab5 (anti-Ara7) (red) on *p35S:GFP-Rab7A1*–expressing root hairs. Endosomes show partial colocalization of anti-Rab5 and GFP-Rab7 (yellow signal; arrow).

(E) Double immunolocalization of anti-Rab7, detected with CY3-tagged secondary antibody (red), and anti-Rab5 (anti-Ara7) detected with Alexa488-tagged secondary antibody (green), on dot-like structures in root hairs of wild-type plants. Rab7 and Rab5 show only partial colocalization (yellow signal).

(F) Immunolocalization of BP-80 (secondary Ab CY3-tagged; red) on *35S:GFP-Rab7A2*–expressing root; note the low level of colocalization. Arrow indicates colocalization.

Bars = 10 μm.

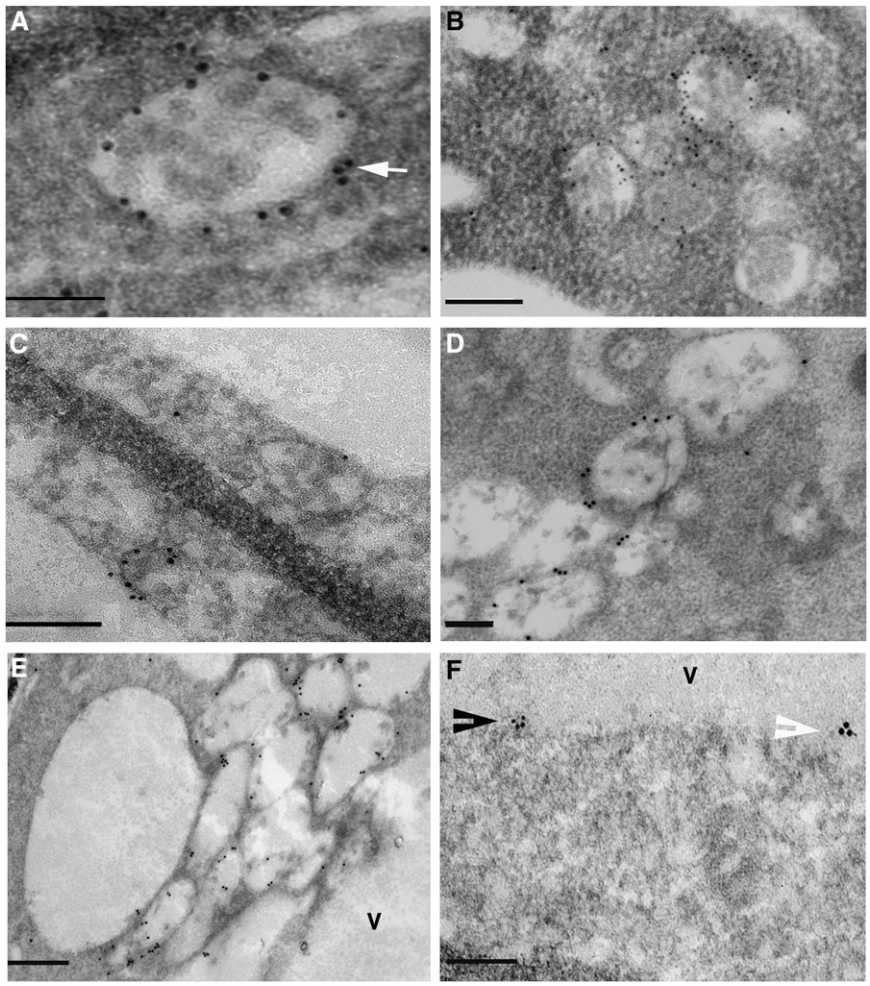

Figure 3. Rab5 and Rab7 Mark Differently Sized MVBs.

(A) and **(B)** EM immunogold detection (immunogold signal appears as black dots; indicated by white arrow) of anti-GFP in *p35S:GFP-Rab5A2*–expressing *Medicago* roots, showing 100- to 300-nm multivesicular endosomes, single **(A)** or in clusters **(B)**.
(C) Anti-Rab5 (anti-Ara7) EM-immunogold detection on *p35S:GFP-Rab5A2* roots shows similarly sized multivesicular endosomes.
(D) and **(E)** EM-immunogold labeling of anti-GFP in *p35S:GFP-Rab7A2*–expressing *Medicago* roots. Immunogold signal is present over 300- to 500-nm MVBs fusing together **(D)** and with the tonoplast **(E)**.
(F) Double immunolocalization on *p35S:GFP-Rab7A2* roots using anti-GFP detected by 15-nm gold particles (white arrowhead) and anti-Rab7 detected by 10-nm gold (black arrowhead). The signal for both GFP and Rab7 is present on the tonoplast. v, vacuole.
Bars = 100 nm in **(A)**, 200 nm in **(B)** to **(D)**, 500 nm in **(E)**, and 200 nm in **(F)**.

(Tse et al., 2004). EM immunogold detection using a Rab5 (anti-Ara7) antibody on transgenic as well as nontransgenic roots confirmed the localization to MVBs with a size of 100 to 300 nm (Figure 3C). This supports our conclusion that the Rab5 fusion proteins are targeted to the same endomembrane compartments (MVBs) as their endogenous counterparts.

Rab7 Marks Endosomes and the Tonoplast

Similar to the Rab5 analyses, GFP-Rab7 fusion constructs for both Rab7A1 and Rab7A2 were expressed under the control of the *35S* promoter or *Ubiquitin3* promoter in *A. rhizogenes*–transformed roots. GFP localization was determined by confocal microscopy in the elongation zone (Figure 1) and root hairs of these roots. GFP fluorescence occurred as mobile dot-like structures in the cytoplasm, which were often in the vicinity of the vacuoles (Figure 1C; see Supplemental Figure 3 online). In addition, small (merging) and large vacuoles were labeled (Figure 1C).

EM immunolocalization of GFP-Rab7A2 (and GFP-Rab7A1), using an antibody against GFP, showed that in both cases, Rab7 associated with the membranes of MVBs ranging in size from 300 to 500 nm (Figures 3D and 3E). In addition, it occurred on the tonoplasts of young (single) vacuoles and clusters of fusing small vacuoles as well as large vacuoles (Figures 3E and 3F).

We verified the localization of endogenous Rab7 to these compartments using anti- *Medicago* Rab7 antibody. In nontransgenic

roots, Rab7 occurred on dot-like structures (Figure 2E) as well as vacuoles. Furthermore, double EM immunolocalization using anti-GFP and anti-Rab7 in the *p35S:GFP-Rab7A2* transgenic roots confirmed their colocalization (Figure 3F). This implies that the GFP fusion construct can be used to identify the endomembrane compartments containing Rab7, and we conclude that Rab7A1/A2 is located on both MVBs (300 to 500 nm) and vacuoles. To determine whether the Rab7-labeled MVBs are part of the endocytic pathway, we also performed a pulse-chase experiment with FM4-64. Colocalization of GFP-Rab7A1/A2 and FM4-64 fluorescence was first seen in dot-like structures (Figure 1D); from 1 h after the FM4-64 pulse colocalization, the tonoplast started to appear, and after ~3 h, the tonoplast was intensely labeled, indicating that also Rab7 MVBs are participating in endocytosis.

Rab5 and Rab7 Occur on Different but Partly Overlapping Endosome Populations

Both Rab5s and Rab7A1/A2 are located on endomembrane compartments (MVBs); however, the Rab7 containing compartments are markedly bigger (300 to 500 nm) than those containing Rab5 (100 to 300 nm). Therefore, it is likely that these MVBs represent distinct populations that only partly overlap. To test this, we performed immunolabeling with anti-Rab5 (anti-Ara7) on transgenic roots expressing GFP-Rab7A1. For analysis, we used root hairs from roots expressing GFP-Rab7A1 as the antibody penetration is better in root hairs and the signal is easy to quantify (Figure 2D). We also performed double immunolocalization with anti-Rab5 (anti-Ara7) and anti-Rab7 on nontransgenic roots (Figure 2E). In both cases, ~30% of the Rab5-labeled dot-like structures colocalized with Rab7-positive structures (Figures 2D and 2E). So the Rab7 endosomes appear to define a unique endocytic compartment.

In *Arabidopsis*, the endocytic pathway and vacuolar biosynthesis pathway merge at Rab5-labeled MVBs, also named PVCs as they contain vacuolar sorting receptors (Li et al., 2002; Paris and Neuhaus, 2002; Jürgens, 2004, Samaj et al., 2005; Foresti et al., 2006). To further characterize the Rab5 and Rab7 MVBs in *Medicago*, we used antibodies against the vacuolar sorting receptor BP-80 (from pea [*Pisum sativum*]), which is generally used as a marker for PVCs in plants (Paris and Neuhaus, 2002). BP-80 occurs in numerous small dots in the cytoplasm, a pattern similar to that of Rab5. Furthermore, in GFP-Rab5A2– or GFP-Rab5B–expressing *Medicago* roots, a high percentage (~80%) of the endosomes contain both BP-80 and Rab5 (Figures 2B and 2C). We also have tested the colocalization of BP-80 with Rab7 MVBs in GFP-Rab7A1 roots. Rab7-positive bodies have a much lower level (<10%) of colocalization with BP-80 compared with Rab5 MVBs (Figure 2F).

So the *Medicago* Rab5 MVBs are very similar to the Rab5 MVBs of *Arabidopsis* as both contain vacuolar sorting receptors. The latter suggests that also in *Medicago* the endocytic pathway and the vacuolar biosynthetic pathway merge at these compartments. Since part of the Rab7-labeled MVBs also contain Rab5, it is possible that they represent an intermediate compartment between Rab5-containing MVBs and vacuoles.

Rab5 Does Not Occur on Symbiosome Membranes

Next, we studied the involvement of the endosomal Rab proteins in symbiosome formation. We first tested whether the Rab5s occur on the symbiosome membrane at any stage of its development.

The cauliflower mosaic virus *35S* promoter was not suitable to visualize GFP fusion constructs during the different stages of symbiosome development, as it is only very weakly active in nodule cells that are infected by rhizobia (Auriac and Timmers, 2007; see Supplemental Figure 4 online). In contrast with the report by Auriac and Timmers (2007), the *35S* promoter used in this study was active in the meristem of the nodule as well as in the uninfected cells (see Supplemental Figure 4 online). The *Arabidopsis Ubiquitin3* promoter is active in the nodule meristem as well as in infected cells of the infection zone, although its activity markedly decreases in the most proximal part of the infection zone. To get stronger fluorescent signal in the infected cells, we additionally used a *Medicago ENOD12* promoter and a pea *leghemoglobin* (*LB*) promoter to express the GFP fusions. *ENOD12* is active in the (distal part of the) infection zone, where bacteria are released from the infection threads and symbiosomes multiply. The *LB* promoter is most active in the fixation zone containing mature, N_2-fixing symbiosomes, but expression already starts in the infection zone. These promoters allowed us to study symbiosomes at all developmental stages.

Rab5 occurred on MVBs in both uninfected and infected cells of root nodules (Figure 4A; see Supplemental Figure 3 online), and this was similar for all three Rab5 homologs. However, none of the three Rab5 fusion proteins colocalized with symbiosomes at any stage of development, from release of the infection thread to mature N_2-fixing symbiosomes. Rab5 proteins were also immunolocalized using anti-Rab5 (anti-Ara7). This confirmed that the Rab5s were present on endosomes (small dot-like structures) in infected and uninfected cells (Figure 4B). However, they were not detected on the symbiosome membrane at any stage of development. Similar results were obtained with immunolocalization of BP-80 in the nodule. Also here, no association of BP-80 with the symbiosome membrane was observed in 14-d-old nodules, whereas BP-80–marked PVCs are present in the infected cells (Figure 4C). Secondary antibody controls did not show any labeling in roots and nodules (see Supplemental Figure 11 online). Also immuno-EM analyses of the transgenic nodules did not show any Rab5 labeling of the symbiosome membrane, whereas a clear signal was observed over endosomes in the same cells. From these data, we conclude that the symbiosome membrane does not acquire the key endocytic marker Rab5 during any stage of symbiosome development.

Rab7 Does Occur on Symbiosome Membranes

In the same way, we examined the localization of Rab7A1/A2 during symbiosome development. As in roots, GFP-Rab7A1/A2 occurs on dot-like endosomes as well as the tonoplast in (un) infected nodule cells (Figures 4D and 4E; see Supplemental Figure 3 online). No labeling of the symbiosome membrane was observed in the distal part of the infection zone, where bacteria are released from the infection thread and symbiosomes are

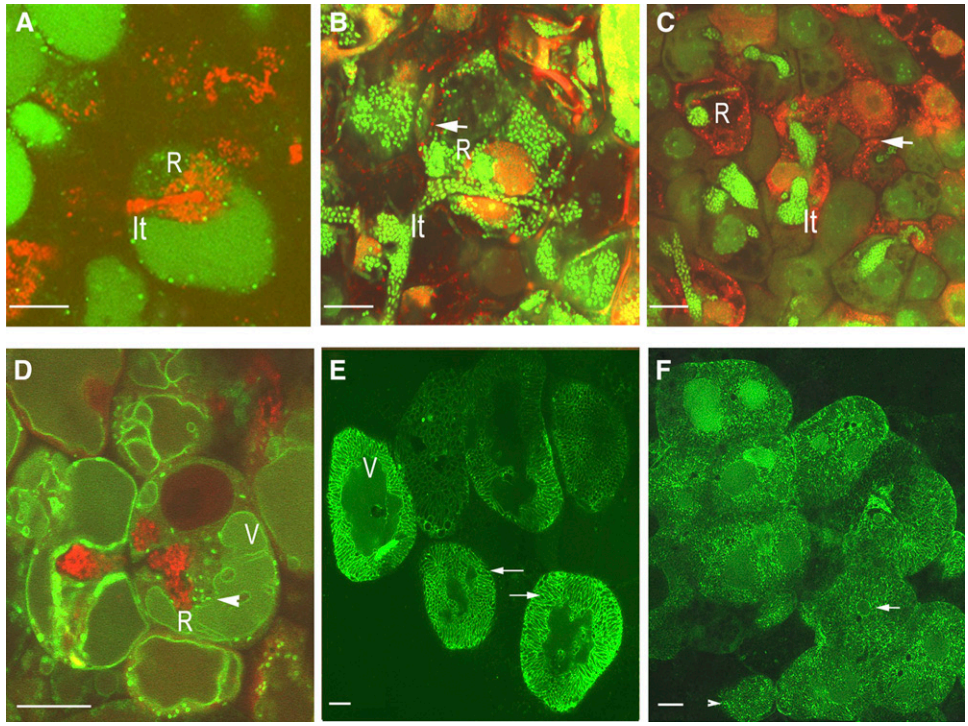

Figure 4. Rab7 Occurs on Symbiosomes, but Rab5 Does Not.

(A) Confocal image of *pUBQ3:GFP-Rab5A2*–expressing nodules. GFP-Rab5A2–labeled endosomes (green dots) are present in the infected cells, but no GFP signal is present on symbiomes after release from the infection thread (It). The rhizobia (R) are expressing monomeric red fluorescent protein (mRFP; red).

(B) Immunolocalization of anti-Rab5 (anti-Ara7) on wild-type nodule-infected cells during symbiosome formation in the infection zone. The signal for Rab5 is revealed as red dots (secondary antibody tagged with CY3; arrow). No colocalization of immunosignal with symbiosomes was observed. The rhizobia are counterstained by Sytox Green.

(C) Immunolocalization of anti-BP80 (red dots [arrow]; CY3-tagged secondary antibody) in the distal infection zone of wild-type nodules. Rhizobia (R) are counterstained by Sytox Green. No colocalization of immunosignal with symbiosomes was observed.

(D) Confocal image of *pE12:GFP-Rab7A2* expression in the distal part of the nodule. GFP-Rab7A2 marks both endosomes and the tonoplast (v, vacuole). No labeling of freshly released symbiomes is seen at this stage. The rhizobia are expressing mRFP (red). R, rhizobia.

(E) Confocal image of *pLB:GFP-Rab7A2* expression in the infection zone of the nodule. The GFP signal is present over the symbiosome membranes of mature symbiosomes (arrow) and the tonoplast. Wild-type bacteria are not counterstained.

(F) Immunolocalization of Rab7 in the fixation zone of wild-type nodules using anti-Rab7. The signal (Alexa488-tagged secondary antibody) is present on symbiosome membranes, tonoplast (arrows), and endosomes (arrowheads).

Bars = 10 μm.

dividing (Figure 4D). However, in the proximal part of the infection zone, where the symbiosomes are elongating and differentiate and in the fixation zone, GFP-Rab7A1/A2 does occur on symbiosome membranes. Rab7 is maintained on symbiosomes throughout the fixation zone (Figure 4E). This was verified by immunolocalizing anti-Rab7 in nontransgenic nodules (Figure 4F). The association of Rab7 with the symbiosome membrane was confirmed by immuno-EM (Figures 5A and 5B). This immunolocalization also confirmed that Rab7 genes are expressed in nodule cells containing symbiosomes.

So our localization studies with the endosomal Rabs showed that symbiosomes do not acquire Rab5, whereas Rab7 is associated with symbiosomes when they start to elongate. The absence of Rab5 on symbiosomes makes it less likely that symbiosomes mature by a sequential interaction with the different compartments of the endocytic pathway. Nevertheless, we tested whether an early endosomal marker is associated with symbiosomes at the stage preceding the presence of Rab7.

To investigate this, we selected a *Medicago* homolog of the *Arabidopsis* SNARE SYP4 family (Mt SYP4; TC96961), which have been shown to mark the TGN (Bassham et al., 2000; Sanderfoot et al., 2001). The TGN was recently shown to function as an early endosome in plants (Dettmer et al., 2006; Robert et al., 2008). We analyzed the localization of GFP-SYP4 in transgenic roots and nodules expressed under the control of the *Ubiquitin3* promoter. In transgenic roots, GFP-SYP4 marks numerous mobile dot-like structures (see Supplemental Figure 5A online), similar to SYP4 proteins in *Arabidopsis*. Furthermore, pulse-chase labeling with FM4-64 in GFP-SYP4 roots showed marked colocalization already within 20 to 30 min after addition

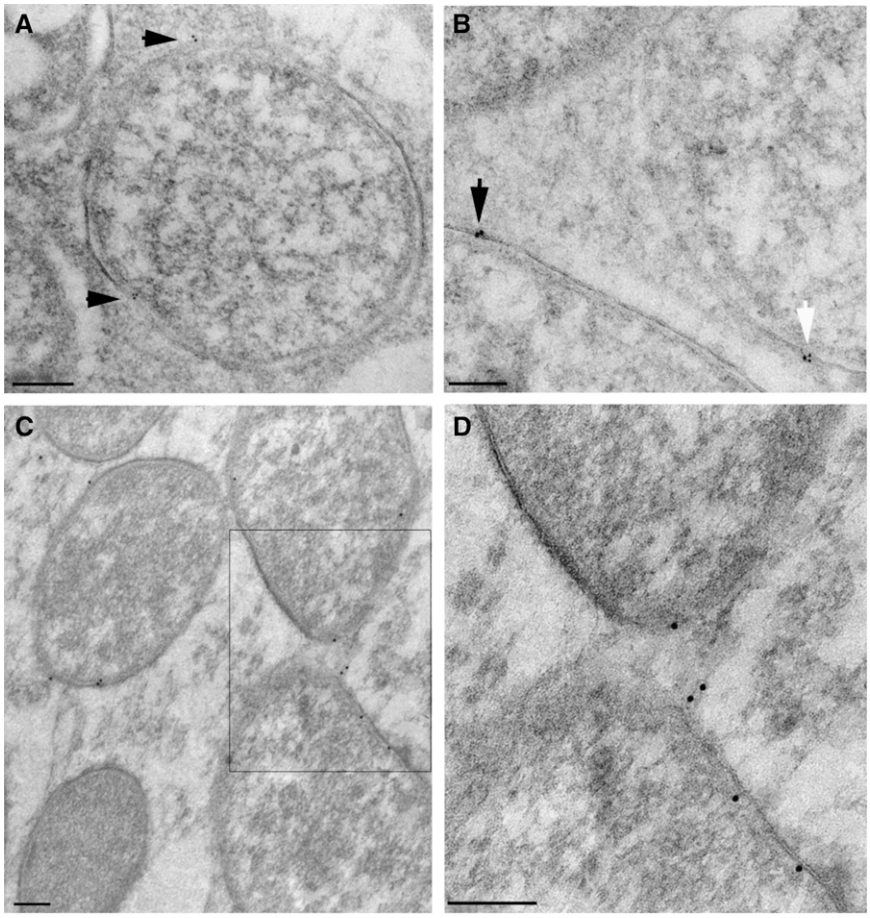

Figure 5. Symbiosome Membranes Contain Rab7 and Acquire SYP22 during Natural Senescence.

(A) Immunogold detection of anti-GFP in *pLB:GFP-Rab7A2*–expressing nodules. The 10-nm gold particles are present over the symbiosome membranes.
(B) Double immunolabeling using anti-GFP (detected by 15-nm gold; black arrowhead) and anti-MtRab7 (10-nm gold; white arrowhead) confirm the presence of Rab7 on the symbiosome membranes.
(C) Immunogold detection of anti-GFP in 5-week-old *pLB:GFP-Syp22*–expressing nodule. The 15-nm gold signal (arrow) is found over the symbiosome membrane in several cells at the base of the nodule.
(D) Close-up of boxed area in **(C)**.
Bars = 500 nm in **(A)** and 200 nm in **(B)** to **(D)**.

of the dye (see Supplemental Figure 5B online). This suggests that *Medicago* SYP4 indeed marks an early endosomal compartment. GFP-SYP4 also marked numerous dot-like structures in infected nodule cells. However, no association with symbiosomes was observed at any stage of development, whereas dot-like structures were labeled in these cells (see Supplemental Figure 5C online). The absence of both SYP4 and Rab5 on symbiosomes makes it unlikely that they acquire Rab7 by sequential interaction with the different compartments of the endocytic pathway.

Functional Analyses of Rab7 in Symbiosome Development

Since Rab7 proteins occur on symbiosomes, we examined whether manipulation of Rab7 activity would interfere with symbiosome development. Therefore, first a dominant-negative construct [T22N] was made locking the protein in the GDP-bound state. Analogous constructs in mammalian cells impair late endosome traffic to lysosomes (Bucci et al., 2000). Expression of *p35S:GFP-Rab7A2[T22N]* in roots resulted in a loss of GFP fluorescence from the endosomes and tonoplast, and instead only cytoplasmic fluorescence was observed (Figure 6A). This indicates that the GFP construct is indeed in a GDP-locked state as such Rab proteins are kept in the cytoplasm through the binding of Rab-GDI factors (Nielsen et al., 2008). However, vacuole formation and root growth were not affected. Similarly, expression of this construct under the control of the nodule-specific *ENOD12* or *LB* promoters did not impair symbiosome development. Also here, GFP fluorescence was only observed in the cytoplasm (Figure 6B). It seems likely that

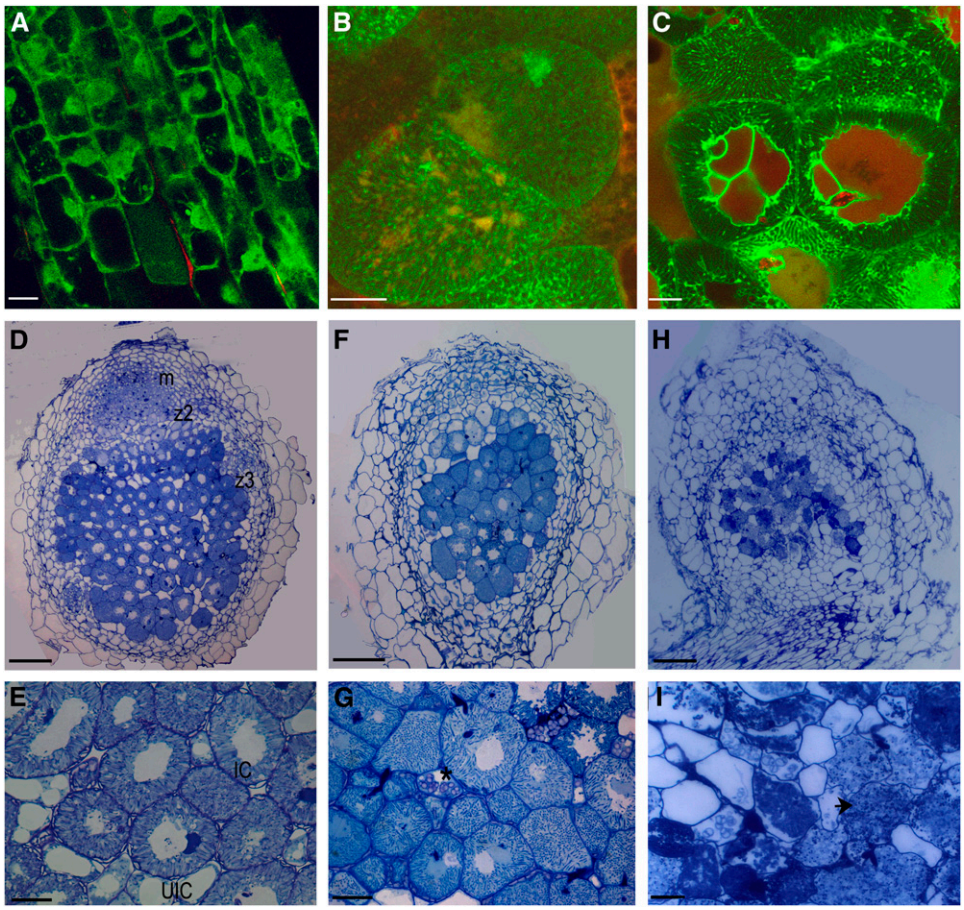

Figure 6. Rab7 Is Required for Symbiosome Development and Maintenance.

(A) Confocal image of dominant-negative *p35S:GFP-Rab7A2[T22N]*–expressing root, showing GFP-Rab7A2[T22N] fluorescence in the cytoplasm.
(B) *pLB:GFP-Rab7A2[T22N]* expression in the nodule also shows fluorescence in the cytoplasm.
(C) Confocal image of constitutively active *pLB:GFP-Rab7A2[Q67L]* –expressing infected cells in a 14-d-old nodule. Stronger labeling of the tonoplast compared to labeling of the symbiosomes can be observed (cf. Figures 6C and 4E). The always-active construct does not induce fusion symbiosomes or their transformation into lytic compartments.
(D) Longitudinal section of a control (empty vector) 14-d-old nodule. Zones: m, meristem; z2, infection zone; z3, fixation zone.
(E) Magnification of z3 in **(D)** showing developed (stage 4) nitrogen-fixing symbiosomes. UIC, uninfected cell; IC, infected cell.
(F) Longitudinal section of a 14-d-old Rab7A1-RNAi nodule.
(G) Magnification of z3 in **(F)**, showing long rod-type (stage 3) symbiosomes present in z3; note intense accumulation of starch grains in noninfected cells (star).
(H) Longitudinal section of a 21-d-old Rab7A1-RNAi nodule showing signs of early senescence; note most of the tissue is degraded.
(I) Magnification of **(H)** showing degraded symbiosomes and dead cells recolonized by saprophytic bacteria (arrow).
Bars = 10 μm in **(A)** to **(C)**, 100 μm in **(D)**, and 50 μm in **(E)**.

expression of the Rab7[T22N] protein was not sufficient to act in a dominant-negative manner as vacuole formation was also not affected.

It is possible that Rab7 activation on the symbiosome membrane is impaired to avoid fusion and formation of lytic compartments. To investigate this possibility, we tested the effect of a constitutively active Rab7 [Q67L] form on symbiosome maintenance. Expression of *p35S:GFP-Rab7A2[Q67L]* in roots did not affect root growth, and GFP fluorescence occurred on the tonoplast as well as on dot-like endosomes (data not shown). In the nodule, we observed a much stronger labeling of the main vacuole compared to symbiosomes in the *pLB:GFP-Rab7A2 [Q67L]* infected cells. By contrast, the tonoplast and symbiosomes are labeled to a similar level in nodules expressing wild-type GFP-Rab7A2. However, symbiosome formation and maintenance as individual units was not affected (Figure 6C). Since active Rab7 is not sufficient to trigger their fusion and formation of lytic compartments, it is probable that components in addition to Rab7 are lacking in the symbiosome membrane.

To further investigate the role of Rab7 in symbiosome development, we knocked down the expression of Rab7A1 using *A. rhizogenes*–mediated RNA interference (RNAi). Rab7A1 RNAi

knocked down the expression of both Rab7A1 and A2 as determined by quantitative RT-PCR analysis (see Supplemental Figure 9 online). No effect on root development was observed. Approximately 65% of the nodules (n = 42) that formed on transgenic Rab7A1 RNAi roots (21 d after inoculation [DAI]) showed an early senescence phenotype (Figures 6D and 6E), in contrast with ~10% of nodules on roots transformed with an empty vector control (n = 24). Since premature senescence is most likely a secondary effect, we studied younger Rab7A1 RNAi nodules (9 and 14 DAI). This showed that symbiosome development in these nodules did not proceed further than stage 3 (elongated rods) (Vasse et al., 1990) and symbiosomes did not reach the mature stage 4 as in control nodules (Figures 6D to 6I), at which they are able to fix atmospheric nitrogen according to Vasse et al. (1990). Instead, premature senescence is induced causing the disintegration of symbiosomes and recolonization of the cells by saprophytic bacteria (Figures 6C and 6I). This shows that symbiosome development becomes arrested at a stage slightly after they normally would acquire Rab7, suggesting that Rab7 is required for the further maturation of the symbiosome.

Syntaxins SYP22, VTI11, and Tonoplast Intrinsic Protein during Symbiosome Development

The presence of Rab7 on the symbiosome membrane suggests that the symbiosome either has the identity of a Rab7-marked MVB or of a young vacuole. To determine whether symbiosomes acquire a vacuolar identity, we analyzed whether other vacuolar identity markers are associated with the symbiosome during its development. A complex of SNAREs SYP22, VTI11, and SYP51 has been suggested to operate at the *Arabidopsis* tonoplast and to control PVC-to-vacuole trafficking (Sanderfoot et al., 2001; Surpin et al., 2003; Yano et al., 2003; Carter et al., 2004; Uemura et al., 2004; Ebine et al., 2008). Therefore, we studied whether the *Medicago* homologs of the vacuolar SNARE proteins, SYP22 and VTI11, occur on symbiosomes.

A *Medicago* SYP22 homolog (TC100656) and VTI11 homolog (TC95338) were fused to GFP and first expressed in transgenic roots under the control of the *Ubiquitin3* promoter. Both GFP-SYP22 (Figures 7A and 7B) and GFP-VTI11 (Figure 7G) located to the tonoplast of young and mature vacuoles and dot-like structures were labeled. The latter might be PVC or even the TGN, as in *Arabidopsis* SYP22 and VTI11 occur on the tonoplast and on PVCs and VTI11 additionally localized to the TGN (Sato et al., 1997; Sanderfoot et al., 1999; Bassham et al., 2000; Uemura et al., 2002, 2004; Carter et al., 2004; Samaj et al., 2005; Sanmartín et al., 2007; Ebine et al., 2008). To confirm the localization of the endogenous proteins, we used anti-*Medicago* VTI11 antibody. Immunolocalization of VTI11 on GFP-SYP22–expressing roots showed a high level of colocalization (see Supplemental Figure 6 online), and the VTI11 antibody marked both the tonoplast and dot-like structures. Therefore, we concluded that the GFP fusion constructs can be used to determine the localization of the endogenous proteins.

As SYP22 (and VTI11) in addition to tonoplast localization is thought to reside at MVBs en route to the vacuole, we examined its localization with respect to Rab7 MVBs. Immunolocalization of RAB7 on GFP-SYP22–expressing roots showed colocalization at the tonoplast as well as a partial colocalization in the dot-like structures (see Supplemental Figure 7 online). This further suggests that Rab7 MVBs are involved in PVC-to-vacuole traffic.

We analyzed the localization of GFP-SYP22 and GFP-VTI11 in relation to symbiosome development in 14-d-old transgenic nodules, expressed either under the control of the *Ubiquitin3* or *LB* promoter. The pattern of localization was similar for both proteins; they occurred on the tonoplast in both infected and noninfected cells (Figures 7A and 7B). However, developing and mature N_2-fixing symbiomes were not labeled by GFP-SYP22 or GFP-VTI11 in 14-d-old nodules (Figures 7C and 7G). So symbiosomes do not have a vacuolar or PVC identity.

In addition to vacuolar SNARE proteins, we also examined the localization of two tonoplast intrinsic protein (TIP) isoforms from *Arabidopsis*: δ-TIP and γ-TIP. γ-TIP was shown to mark the lytic vacuole in plants, while δ-TIP was shown to additionally mark storage-type vacuoles in vegetative cells (Jauh et al., 1999). GFP-γ-TIP and GFP-δ-TIP expressed under control of the *Ubiquitin3* promoter both labeled the main vacuole in root and nodule cells (Figures 7E and 7F). However, they both do not occur on the symbiosome membrane in young infected cells, supporting the conclusion that symbiosomes do not have a vacuolar identity.

When nodules become older (from ~4 weeks after inoculation) they start to senesce, which starts with the fusion and formation of lytic symbiosome compartments in the most proximal (oldest) infected cells (Vasse et al., 1990; Van de Velde et al., 2006). This fusion of symbiosomes to form lytic compartments resembles vacuole formation. Therefore, we wondered whether the symbiosomes at this stage acquire vacuolar identity. Indeed, in 5-week-old nodules, GFP-SYP22 and GFP-VTI11 do occur on the symbiosome membrane in cells in the proximal part of the nodule closest to the root (Figure 7D). In certain cells, actually part of the symbiosomes show labeling of the symbiosome membrane, while other symbiosomes in the same cell have not yet acquired the vacuolar markers (Figure 7D). This likely represents a very early stage of senescence. The association of endogenous VTI11 with symbiosomes during senescence was confirmed using the VTI11 antibody on 8-week-old wild-type nodules (Figure 7H). Rab7 is also still associated with symbiosomes during senescence (data not shown). Immuno-EM analysis of GFP-SYP22 senescent transgenic nodules confirmed that GFP-SYP22 now marks the symbiosome membrane (Figures 5C and 5D).

In Rab7 RNAi roots, neither vacuole formation nor symbiosome senescence is blocked. Therefore, we assumed that the vacuolar syntaxins are still targeted to their membranes despite the reduced levels of Rab7. Immunolocalization of anti-VTI11 in Rab7A1 RNAi roots showed that VTI11 indeed occurs on the tonoplast and endosomes, like in wild-type plants (see Supplemental Figure 8A online). Furthermore, in the Rab7A1 RNAi nodules, senescing symbiosomes do contain VTI11 (see Supplemental Figure 8B online), indicating the senescence-related acquisition of vacuolar identity.

These observations suggest that the survival and maintenance of the bacteria in individual symbiosome compartments during the N_2-fixing stage is achieved by delaying the acquisition of vacuolar identity (e.g., vacuolar SNAREs).

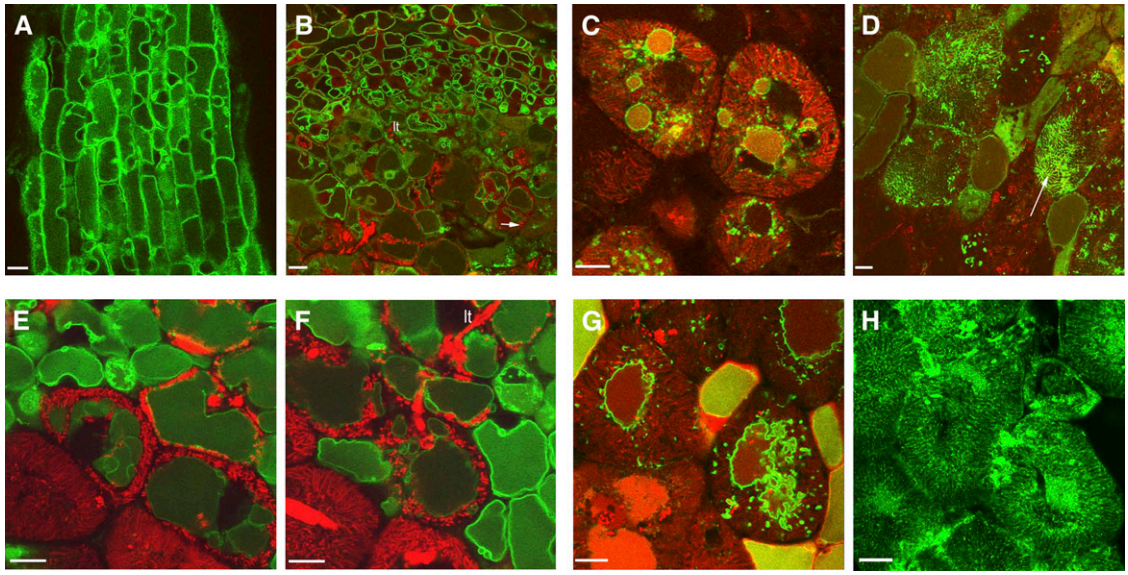

Figure 7. Symbiosomes Do Not Have Vacuolar Identity until the Onset of Senescence.

(A) Confocal image of *pUBQ3:GFP-MtSYP22*–expressing root, showing mainly tonoplast labeling.
(B) Confocal image of *pUBQ3:GFP-MtSYP22*–expressing 14 DAI nodule, showing tonoplast labeling. No signal is observed on the symbiosomes (arrow).
(C) *pLB:GFP-MtSYP22* expression in the infected cells of the fixation zone of 14 DAI nodules. GFP-MtSYP22 appears on the tonoplast and dot-like structures, but not on the symbiosomes.
(D) In 5-week-old *pLB:GFP-MtSYP22*–expressing nodules, GFP-MtSYP22 can be observed over the senescent symbiosome membrane (arrow) in the basal part of the nodule.
(E) Confocal image of *pUBQ3:At-γ-TIP-GFP*–expressing 14-d-old nodule, showing labeling of the tonoplast, but not of the young differentiating symbiosomes.
(F) *pUBQ3:At-δ-TIP-GFP*–expressing 14-d-old nodule, showing also tonoplast but not symbiosome labeling.
(G) Confocal image of *pLB:GFP-MtVTI11* expression in the infected cells of the fixation zone of 14 DAI nodules. In contrast with tonoplast labeling, symbiosomes are not labeled.
(H) Immunolocalization of MtVTI11 on 8-week-old wild-type nodule tissue showing the labeling of symbiosome membranes in senescent nodules.
Rhizobia in **(B)** to **(F)** are expressing mRFP (red). It, infection thread. Bars = 500 nm in **(A)** and 200 nm in **(B)** to **(D)**.

The Plasma Membrane SNARE SYP132 Occurs on Symbiosomes throughout Their Development

A proteomics approach has previously identified a plasma membrane syntaxin, SYP132 (TC86779), which immunolocalized to the infection thread membrane as well as to the symbiosome membrane, although it was not reported from which developmental stage (Catalano et al., 2007). Therefore, we wondered whether early symbiosomes (directly after release from the infection threads) contain this syntaxin and whether they retain this marker during further development. We created a GFP fusion construct and studied its localization in roots and nodules. In roots, GFP-SYP132 marks the plasma membrane and occasionally accumulates in spots in the plasma membrane (Figure 8A). In nodules, GFP-SYP132 marks the plasma membrane as well as the infection thread membrane (Figure 8B) and labels the symbiosome membrane as soon as the rhizobia are taken up into the cells (Figures 8B and 8C). GFP-SYP132 strikingly labels the symbiosome membrane throughout all developmental stages up to stage 4 in the fixation zone (Figure 8D) as well as during senescent stages. Therefore, mature symbiosomes appear to have a unique mosaic identity, containing both SYP132 and Rab7.

DISCUSSION

We showed that the *Medicago* Rab5s and Rab7A1/A2 are late endosomal membrane identity markers. The latter mark a unique endomembrane compartment in plants that might be positioned in between Rab5 MVBs and the vacuole. Symbiosomes do not contain Rab5s at any stage of their development and the TGN marker SYP4, thought to be an early endosome marker, did not occur on symbiosomes. By contrast, Rab7 is acquired by symbiosomes when they have stopped dividing and start to elongate, and it is maintained up to the senescence stage. However, the symbiosomes do not acquire a (lytic) vacuole identity (vacuolar SNAREs) until the onset of senescence. Instead, symbiosomes acquire the plasma membrane SNARE SYP132 from the start of symbiosome formation throughout their development. Therefore, symbiosomes appear to be locked in a unique SYP132 and Rab7 positive stage, and the delay in acquiring vacuolar identity most likely facilitates their maintenance as individual membrane compartments.

The membrane identity markers used in this study were selected based on homology to well-studied *Arabidopsis* counterparts as well as on their expression in infected cells of the

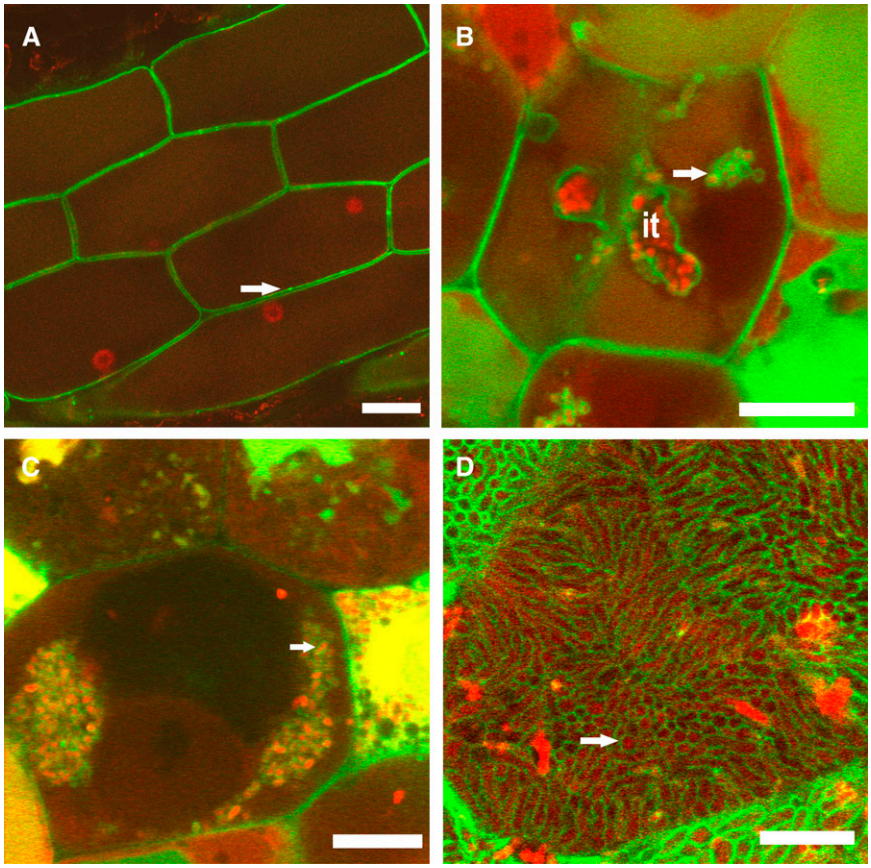

Figure 8. Symbiosomes Retain Plasma Membrane Identity throughout Their Development.

(A) Confocal image of *pUBQ:GFP-SYP132*–expressing root. GFP-SYP132 marks the plasma membrane and occasionally accumulates in spot in the plasma membrane (arrow).
(B) and **(C)** *pE12:GFP-SYP132*–expressing nodules show GFP-SYP132 on the plasma membrane and infection thread (it) membrane as well as just formed symbiosomes (**[B]**; arrow) and early stage symbiosomes (**[C]**; arrow).
(D) *pLB:GFP-SYP132*–expressing nodule showing GFP-SYP132 marking the symbiosome membrane (arrow) in fully infected cells of the fixation zone. Rhizobia in **(B)** to **(D)** are expressing mRFP (red).
Bars = 20 μm **(A)** and 10 μm in **(B)** to **(D)**.

nodule, which was confirmed by microarray analysis on RNA from infected cells isolated by laser microdissection. Specific antibodies for Rab5, Rab7, and VTI11 confirm that the corresponding genes are indeed active in the infected as well as uninfected cells of *Medicago* nodules and that the GFP fusion constructs correctly mark the localization of the endogenous proteins.

Medicago has three Rab5 homologs, similar to *Arabidopsis*. These Rab5 proteins mark multivesicular endosomes (100 to 300 nm) in *Medicago* root and nodule cells. The high level of colocalization of these Rab5 endosomes with the (lytic) vacuolar sorting receptor BP-80 identifies them as PVCs, similar as in *Arabidopsis* (Paris and Neuhaus, 2002; Sohn et al., 2003; Foresti et al., 2006; Lam et al., 2007). Labeling by the endosomal tracer FM4-64 shows that the Rab5 MVBs are involved in endocytosis. Therefore, it is very probable that like in *Arabidopsis* (and yeast), the endocytic and vacuolar transport pathways merge at these Rab5-labeled MVBs (Gerrard et al., 2000; Pelham, 2002; Tse et al., 2004; Lam et al., 2007; Jaillais et al., 2008; Robinson et al., 2008). *Medicago* Rab7A1/A2 is located at 300 to 500 nm MVBs that become labeled with the endocytic tracer FM4-64 as well as the tonoplast. The latter has also been observed in rice and *Arabidopsis* (Saito et al., 2002; Nahm et al., 2003). Interestingly, the involvement of Rab7-labeled MVBs in endocytosis in plants raises the possibility that, like in mammalian cells, Rab5-labeled MVBs mature into Rab7 MVBs that subsequently fuse with a lytic compartment (Rink et al., 2005; Vonderheit and Helenius, 2005). In this case, the Rab7 MVBs function as a transitory compartment between Rab5 late endosomes and the vacuole, like in yeast (Pelham, 2002). Consistent with this hypothesis is the observed colocalization of Rab5 and Rab7 in ~30% of the endosomes and the markedly bigger size of Rab7-labeled MVBs compared to Rab5 MVBs, as in animals (Méresse et al., 1995). Colocalization of BP-80 with Rab7 showed markedly less colocalization than BP-80 with Rab5 and Rab7. This might suggest that vacuolar sorting receptors are recycled from the Rab5

MVBs, as these mature to Rab7 MVBs. However, in vivo studies on maturating endosomes remain to be done in *Medicago* to prove that Rab5 MVBs mature via Rab7 MVBs. With the current knowledge, it cannot be excluded that Rab7-labeled endosomes are involved in a Rab5-independent endocytic pathway.

Symbiosomes do not acquire Rab5s at any stage of their development into mature N_2-fixing organelles. Also BP-80, which colocalizes with Rab5 on endosomes, does not occur on symbiosome membranes. Even at the stage where Rab7 does not yet occur at the symbiosome membrane, Rab5 and BP-80 are not present. At this stage, symbiosomes also do not show any association of the early endosome marker SYP4. Therefore, it is unlikely that symbiosome formation involves fusion with the TGN or Rab5 endosomes, although these are present in the infected nodule cells.

By contrast, the symbiosome membrane acquires the endosomal/vacuolar marker Rab7A1/A2 when symbiosomes have stopped dividing. This suggests that symbiosomes either have vacuolar identity or Rab7-MVB identity. The absence of the vacuolar syntaxins SYP22 and VTI11 up to the senescence stage suggests that a Rab7-MVB identity is more probable. So although our studies suggest that the Rab5- and Rab7-labeled endosomes can be part of the same endocytic pathway, Rab7 is recruited to the symbiosome membrane in a Rab5-independent manner. In this case, early steps of symbiosome formation are not related to the Rab5-dependent endocytic pathway. It appears that early steps of symbiosome formation do not require any endocytic machinery, and Rab7 might be recruited directly from the cytoplasm to facilitate symbiosome development. An endocytosis-independent process would be consistent with the presence of the plasma membrane–type syntaxin, SYP132, on the symbiosome membrane throughout its development. The combined presence of SYP132 and Rab7 suggests a unique mosaic identity of the symbiosome membrane, which could allow the bacteria to intercept both specific secretory traffic to the plasma membrane and specific endocytic/biosynthetic traffic towards the vacuole. Generally during endocytosis, plasma membrane identity markers are recycled/removed as endocytic vesicles are sorted along the endocytic pathway. Therefore, retaining SYP132 on the symbiosome membrane suggests either an endocytosis-independent process or a block of recycling of SYP132 during endocytosis. We are currently investigating the role of the plasma membrane–directed secretory pathway in symbiosome formation and development.

On the other hand, it is possible that Rab7-labeled endosomes are involved in a yet uncharacterized Rab5-independent endocytic pathway, suggesting the existence of additional not yet characterized endosome compartments in plants. Theoretically, developing symbiosomes might interact with these endosomes before acquiring Rab7. In animal cells, non-Rab5–labeled early endosomes have been identified that are associated with lipid raft/nonclathrin-mediated endocytosis in a pathway that does not lead to fusion with lysosomes (Conrad et al., 1995; Shin and Abraham, 2001; Mayor and Pagano, 2007).

Several pathogenic bacteria that are able to survive in vacuole-like compartments in animal cells, such as *Legionella pneumophila* and *Escherichia coli*, have also been shown to acquire the late endosomal marker Rab7 in a Rab5-independent manner (Clemens et al., 2000a, 2000b; Shin et al., 2000; Passey et al., 2008). Like symbiosomes, both are maintained as individual compartments that do not fuse with lysosomes, indicating that Rab7 is not sufficient to induce fusion with a lytic compartment. Even association of constitutively active GTP-locked GFP-Rab7A2[Q67L] with the symbiosome membranes did not induce their fusion and formation of lytic compartments. By contrast, stronger labeling of the tonoplast was observed in the infected cells expressing GFP-Rab7A2[Q67L] compared to symbiosome labeling. This might indicate that there is enhanced trafficking from Rab7 endosomes to the vacuole similar as in animal cells where always-active forms of Rab7 indeed enhance endocytic traffic to lysosomes (Méresse et al., 1995). Similarly, in *Legionella*- or *Salmonella*-infected animal cells, the presence of an always-active Rab7 on the bacteria-containing membrane compartments is not sufficient to promote their fusion with lysosomes (Clemens et al., 2000a; Harrison et al., 2004). Therefore, components required in addition to Rab7 to facilitate fusion and the transition into a lytic compartment are missing in the symbiosome membrane (Vieira et al., 2003).

Vacuolar SNARE proteins play a role in vacuole biogenesis and do occur in plant PVCs and tonoplast (Sato et al., 1997; Sanderfoot et al., 1999, 2001; Rojo et al., 2003; Carter et al., 2004; Samaj et al., 2005; Bassham and Blatt, 2008; Ebine et al., 2008). Therefore, we studied the vacuolar SNAREs SYP22 and VTI11 and showed that they occur on the tonoplast (and likely PVCs) of root cells as well as of infected and uninfected nodule cells. However, they do not occur on young symbiosomes and only appear on the symbiosome membrane as senescence starts, when symbiosomes fuse and form lytic compartments (Van de Velde et al., 2006). This process resembles lytic vacuole formation, which fits with the observation that the vacuolar identity markers SYP22 and VTI11 now mark the symbiosome membrane. Therefore, we propose that the delay in acquiring lytic vacuolar identity (e.g., vacuolar SNARE proteins) by the symbiosomes is facilitating maintenance of symbiosomes as individual N_2-fixing organelles. How this delay is established remains to be solved.

It has previously been suggested that symbiosomes represent vacuole-like compartments in analogy to protein storage vacuoles (PSVs) (Mellor, 1989). Lytic vacuoles and storage-type vacuoles can be distinguished by the respective presence of the vacuolar-targeted TIP proteins γ-TIP and δ-TIP (Jauh et al., 1999). The absence of both γ-TIP and δ-TIP on functional symbiosomes suggests that symbiosomes do not have lytic or storage vacuole identity, although we did not study whether these TIP proteins indeed distinguish PSVs from lytic vacuoles in *Medicago*. During seed germination, PSVs are thought to acquire lytic activity through the delivery of newly formed proteases via MVBs (Wang et al., 2007). Comparably, the observed acquisition of vacuolar identity by symbiosomes upon senescence likely allows the delivery of newly formed proteases to facilitate the switch to lytic compartments.

Our data indicate that Rab7 is not essential for proper localization of vacuolar SNAREs, as VTI11 localization was not affected in Rab7A1 RNAi roots or in nodule cells that show an early senescence phenotype. However, redundant roles of additional members of the Rab7 family cannot be ruled out, as in

Arabidopsis double, triple, and quadruple Rab7 mutants did not show obvious phenotypes (T. Ueda, unpublished data in Nielsen et al., 2008). A study in soybean had previously shown that antisense expression of a Rab7 homolog resulted in a more frequent degradation of symbiosomes in vacuole-like compartments (Cheon et al., 1993). However, in this study, the leghemoglobin promoter was used to drive the antisense construct by which it is first expressed at a late stage of development. Here, we show that knockdown of Rab7A1/A2 expression actually blocked symbiosome development at a stage where symbiosomes had started elongation (differentiation) but were not yet fixing nitrogen. This suggests that Rab7 is essential for proper development into a nitrogen-fixing organelle. How Rab7 regulates symbiosome development and maintenance remains unclear. It is possible that unknown components required for symbiosome development/maintenance require Rab7 for proper targeting to the symbiosomes.

The Rab7 endosomal nature of symbiosomes might explain the reported presence of several vacuolar enzymes in the symbiosome space (Mellor, 1989; Jones et al., 2007), as these are likely transported to the vacuole via late endosomes. This is further supported by the observation that a Cys protease, which localizes to the symbiosome space, is indeed detected in both vacuoles and ~500-nm cytoplasmic vesicles in pea roots and nodules (Vincent and Brewin, 2000). Although the nature of these ~500-nm cytoplasmic vesicles was not studied, their ultrastructure seems strikingly similar to the Rab7-MVB.

In conclusion, symbiosome development appears to involve only part of the known/default endocytic machinery, and this is first used when symbiomes stop dividing. Which endomembrane processes have been adapted to support the endocytotic uptake of rhizobia in nodule cells and the subsequent proliferation of symbiosomes remains to be revealed. The continued presence of SYP132 during symbiosome development suggests a major role for the secretory pathway. Furthermore, Rab7-containing symbiosomes are maintained as individual N_2-fixing compartments by delaying the acquisition of (lytic) vacuolar identity. Therefore, it will be important to determine the molecular mechanism by which this is achieved.

METHODS

Plant Transformation and Rhizobial Strains

The *Medicago truncatula* accession Jemalong A17 was used. *Agrobacterium rhizogenes* strain MSU440 (Sonti et al., 1995) was used for hairy root transformations according to Limpens et al. (2004). For nodulation, *Sinorhizobium meliloti* strain Sm2011 or *S. meliloti* Sm2011-mRFP (Smit et al., 2005) expressing the red fluorescent mRFP protein were used. Nodulation was done according to Limpens et al. (2004) using 2 mL (OD_{600} 0.1) rhizobial suspension per plant.

Constructs

Medicago Rab5A1, *A2*, and *B* and *Rab7A1*, *A2*, *SYP22*, *VTI11*, *SYP132*, and *SYP4* open reading frames were PCR amplified from 10-d-old nodule cDNA using Phusion high fidelity Taq polymerase (New England Biolabs) and directionally cloned into pENTR-D-TOPO (Invitrogen). PCR primers are presented in Supplemental Table 1 online. *Medicago SYP22* and *VTI11* were directionally cloned with *Hin*dIII-*Kpn*I and *Bam*HI-*Eco*RI, respectively, into a modified pENTR vector (pENTR2) containing a multiple cloning site. *Arabidopsis thaliana* δ-*TIP* (NM_112495) and γ-*TIP* (NM_129238) were amplified from *Arabidopsis* Columbia root cDNA and cloned *Bam*HI-*Eco*RI into pENTR2. pENTR clones Rab5A1, Rab5A2, Rab7A1, Rab7A2, SYP22, VTI11, SYP132, and SYP4 were recombined into either of the following Gateway-compatible binary vectors using LR Clonase (Invitrogen): 35S-pK7WGF2-R (containing the 35S promoter) (Smit et al., 2005), UBQ3-pK7WGF2-R, E12-pK7WGF2-R, and LB-pK7WGF2-R, creating N-terminal GFP-X fusions. pENTR clone Rab5B was recombined into 35S-pK7FWG2 (Karimi et al., 2002), E12-pK7FWG2, and LB-pK7FWG2; pENTR clones δ-TIP and γ-TIP were recombined into UBQ3-pK7FWG2, creating C-terminal X-GFP fusions. For RNAi, pENTR-Rab7A1 was recombined into pK7GWIWG2(II)-Q10:DsRED (Limpens et al., 2005). All constructs were verified by sequencing and restriction digestion. The constructs were transformed to MSU440 and used for hairy root transformations.

Constitutive-active [Q67L] and dominant-negative [T22N] *Rab7A2* constructs were generated via two subsequent PCR reactions using Rab7A2-F x Rab7A2[Q67L]-2/Rab7A2[T22N]-2 and Rab7A2-R x Rab7A2 [Q67L]-1/Rab7A2[T22N]-1 in a first PCR reaction using Phusion high fidelity Taq polymerase (New England Biolobs). PCR primers are presented in Supplemental Table 1 online. The obtained fragments were diluted 1:1000 and used in a second PCR reaction using Rab7A2-F and Rab7A2-R. The resulting fragment was directionally cloned into pENTR-D-TOPO (Invitrogen), verified by sequencing, and subsequently recombined into 35S-pK7WGF2-R, E12-pK7WGF2-R, and LB-pK7WGF2-R.

The Gateway-compatible binary vectors containing the *Ubiquitin3* (UBQ3), *ENOD12* (E12), and pea (*Pisum sativum*) LB promoters were created by digesting pK7FWG2 (Karimi et al., 2002) or pK7WGF2-R (Smit et al., 2005) with *Hin*dIII-*Spe*I (removing the 35S promoter) and ligating the corresponding promoter fragments amplified using specific primers, which are presented in Supplemental Table 1 online.

Quantitative PCR Analysis

Quantitative RT-PCR was conducted on RNA isolated form nitrogen-starved, uninoculated roots, 10-d-old nodules, and 3-week-old nodules as well as on RNA from nodulated Rab7A1 RNAi and control roots. Total RNA was isolated and DNAse treated using the Plant RNeasy kit (Qiagen; according to the manufacturer's instructions). cDNA was synthesized from 1 μg total RNA using the Taqman Gold RT-PCR kit (Perkin-Elmer Applied Biosystems) in a total volume of 50 μL using random hexamer primers (10 min 25°C, 30 min 48°C, and 5 min 95°C) . Quantitative PCR reactions were performed in triplicate on 1 μL cDNA using the Quantitative PCR Core kit for SYBR Green I (Eurogentec), and real-time detection was performed on a MyiQ (Bio-Rad) (40 cycles of 95°C for 10 s and 60°C for 1 min) followed by a heat dissociation step (from 65 to 95°C). Primers were used at a final concentration of 300 nM. *GAPDH* was used as reference. PCR primers are presented in Supplemental Table 1 online.

Fluorescence Microscopy

Transgenic roots and nodules were selected based on GFP or DsRED1 expression using a Leica MZFLIII binocular fitted with HQ470/40, HQ525/50, HQ553/30, and HQ620/60 optical filters (Leica Microsystems). Transgenic nodules were hand-sectioned using double-edged razorblades and mounted on microscope slides in 0.1 M phosphate buffer, pH 7.4, containing 25 mg/mL sucrose. Transgenic roots and sectioned nodules were further analyzed on a Zeiss LSM 510 confocal laser scanning microscope (Carl-Zeiss Axiovert 100 M equipped with a LSM510, an argon laser with a 488-nm laser line, a helium-neon laser with a 543-nm laser line); excitation at 488 nm (GFP; Sytox Green/Alexa 488) and 543 nm

(DsRED1/mRFP/CY3); GFP/Sytox Green/Alexa 588 emission was selectively detected using a 505- to 530-nm band-pass filter; DsRED1/mRFP/CY3 emission was detected in another channel using a 560- to 615-nm band-pass filter.

Immunolocalization

Nodules were hand-sectioned using a double-edged razorblade. Nodule sections or roots were fixed in 1% of freshly depolymerized paraformaldehyde in 1× PBS, pH 7.4, for 30 min at 4°C. Nodule sections were blocked in normal goat serum or 3% BSA and further incubated with the primary antibody overnight at 4°C in 1× PBS containing 0.3% Triton X-100. The secondary antibodies anti-Rabbit Alexa 488, anti-mouse Alexa 488, anti-Mouse CY3 (Molecular Probes) were used according to the supplier's instructions. Controls were carried out in the absence of primary antibodies. Nodule sections containing wild-type Sm2011 rhizobia were counterstained with Sytox Green (Molecular Probes) or propidium iodide and examined by confocal microscopy. Primary antibody dilutions were as follows: anti-GFP rabbit (Molecular Probes), 1:200; anti-GFP mouse (Molecular Probes), 1:50; anti-Ara7 (T. Ueda), 1:200; anti-Ara6 (T. Ueda), 1:100; anti-Rab7 mouse (GenScript), 1:50 and 1:100; anti-VTI11 (rabbit) (GenScript), 1:100 and 1:200; anti-BP-80 (N. Paris), 1:100. Affinity-purified polyclonal mouse anti-Rab7 and polyclonal rabbit anti-VTI11 were generated by GenScript against the peptides FLIQANPSDPENFPC (Rab7) and RKMDLEARSLQPNIC (VTI11).

FM4-64 Staining

Transgenic roots were selected using the Leica MZFLIII fluorescence stereomacroscope, cut from the plant, and directly placed into a solution of FM4-64 (30 μg/mL) in phosphate buffer (0.1 M, containing 25 mg/mL sucrose) on ice for a minimum period of 30 min. The roots were washed two times in phosphate buffer (0.1 M, containing 25 mg/mL sucrose) to remove the excess FM4-64 and incubated at room temperature for the indicated times.

EM Sample Preparation by High-Pressure Freezing and Freeze Substitution

For tissue processing, a modified method of Thijssen et al. (1997) was used. Nodules and roots were cryofixed with a Balzers HPM 010 high-pressure freezing device, and specimens were further placed in heptane. Freeze substitution was performed with a FreasySub unit (Cryotech Benelux, Schagen-NL), from −90 to 0°C for 68 h. The substitution medium contained 0.3% glutaraldehyde + 0.2% uranyl acetate in acetone. Samples were embedded in LR White resin with 0.5% benzoin methyl ether as a catalyst and polymerized under UV light at −20°C. Some samples were fixed by a conventional method in 4% paraformaldehyde mixed with 0.3% glutaraldehyde in 50 mM phosphate buffer, pH 7.4, embedded in LR white resin prepared as above and polymerized with UV light at −20°C.

For the analysis of the structure of Rab7A1 RNAi nodules, the tissue was fixed by the conventional method in 4% paraformaldehyde with 3% glutaraldehyde in 50 mM phosphate buffer, pH 7.4, postfixed with 1% OsO_4, embedded in LR white resin according to the supplier's recommendations and polymerized at 60°C.

EM Immunodetection

Thin sections (60 nm) were cut using a Leica Ultracut microtome. Nickel grids with the sections were blocked in normal goat serum or 2% BSA in PBS. Grids were incubated overnight at 4°C with the primary antibody according to dilutions given above. Goat anti-rabbit coupled with 15-nm gold (BioCell) (1:50 dilution), donkey anti-rabbit (15 nm) (1:50), or donkey anti-mouse coupled with 10-nm gold (1:30) (Aurion) was used as secondary antibody. The sections were contrasted with 2% aqueous uranyl acetate and lead citrate and examined using a JEOL JEM 2100 transmission electron microscope equipped with a Gatan US4000 4K × 4K camera.

Phylogenetic Analyses

Phylogenetic analyses were conducted using MEGA version 4 (Tamura, Dudley, Nei, and Kumar 2007). A multiple protein alignment was made using default parameters: gap opening, 10.00; gap extension, 0.20; residue-specific penalties, on; hydrophilic penalties, on; gap separation distance, 4; end gap separation, off; negative matrix, off; delay divergent sequences, 30%; protein weight matrix, Gonnet Series. The alignment is provided in Supplemental Data Set 1 online. From this alignment a midpoint-rooted neighbor-joining tree with bootstraps values (1000 replicates) was drawn.

Accession Numbers

Sequence data from this article can be found in the GenBank/EMBL data libraries or TIGR Gene Indices under the following accession numbers: Rab5A1, TC106962; Rab5A2, TC106963; Rab5B, TC93994; Rab7A1, TC101145; Rab7A2, TC94423; SYP4, TC96961; VTI11, TC95338; SYP22, TC100656; SYP132, TC86779; GAPDH, BT052418.1; *Arabidopsis* δ-TIP, NM_112495; *Arabidopsis* γ-TIP, NM_129238.

Supplemental Data

The following materials are available in the online version of this article.

Figure 1. Phylogenetic Comparison of Rab5 and Rab7 Proteins from *Medicago* and *Arabidopsis*.

Figure 2. Quantification of Rab5A1, A2, and B, and Rab7A1 and A2 Expression Levels in Roots, 10-d-Old Nodules, and 3-Week-Old Nodules.

Figure 3. Confocal Images of GFP-Rab5A1, GFP-Rab5B, and GFP-Rab7A1 in Roots and Nodules.

Figure 4. Confocal Image of a *Medicago* Nodule Expressing *p35S: GFP-Rab7A2[Q67L].*

Figure 5. Localization of GFP-SYP4 in Roots and Nodules.

Figure 6. Immunolocalization of VTI 11 on GFP-SYP22 Roots.

Figure 7. Immunolocalization of Rab7 on GFP-SYP22 Roots.

Figure 8. Immunolocalization of VTI11 on Rab7A1 RNAi Roots and Nodules.

Figure 9. Quantification of *Rab7A1* and *Rab7A2* Knockdown Levels in Rab7A1-RNAi Nodulated Roots.

Figure 10. Preimmune (Mouse Preimmune Serum) Control for Anti-Rab7Ab.

Figure 11. Secondary Antibody (Anti-Mouse CY3) Control on Wild-Type Nodules.

Supplemental Table 1. Primers Used in This Study.

Supplemental Data Set 1. Text File of Alignment Used for Phylogenetic Tree in Supplemental Figure 1.

ACKNOWLEDGEMENTS

We thank Takashi Ueda for kindly providing the anti-Ara7 antibody and Nadine Paris for the anti-BP-80 antibody. We are grateful for technical support from A.C. Van Aelst and T. Fransen in high-pressure freezing

preparation of EM samples. EM imaging and sample preparation were performed at the Wageningen Electron Microscopy Center (Wageningen University). This study was supported by a The Netherlands Organization for Scientific Research/Russian Federation for Basic Research grant for Centre of Excellence 047.018.001 and NWO Grant 3184319448.

Received November 17, 2008; revised July 30, 2009; accepted August 14, 2009; published September 4, 2009.

REFERENCES

Alonso, A., and Garcia-del Portillo, F. (2004). Hijacking of eukaryotic functions by intracellular bacterial pathogens. Int. Microbiol. **7:** 181–191.

Auriac, M.-C., and Timmers, A.C.J. (2007). Nodulation studies in the model legume *Medicago truncatula*: Advantages of using the constitutive EF1α promoter and limitations in detecting fluorescent reporter proteins in nodule tissues. Mol. Plant Microbe Interact. **20:** 1040–1047.

Bassham, D.C., and Blatt, M.R. (2008). SNAREs: Cogs and coordinators in signaling and development. Plant Physiol. **147:** 1504–1515.

Bassham, D.C., and Raikhel, R.V. (2000). Unique features of the plant vacuolar sorting machinery. Curr. Opin. Cell Biol. **12:** 491–495.

Behnia, R., and Munro, S. (2005). Organelle identity and the signposts for membrane traffic. Nature **438:** 597–604.

Bolte, S., Brown, S., and Satiat-Jeunemaitre, B. (2004). The N-myristoylated Rab-GTPase m-Rabmc is involved in post-Golgi trafficking events to the lytic vacuole in plant cells. J. Cell Sci. **117:** 943–954.

Bruckert, F., Laurent, O., and Satre, M. (2000). Rab7, a multifaceted GTP-binding protein regulating access to degradative compartments in eukaryotic cells. Protoplasma **210:** 108–116.

Brumell, J.H., and Grinstein, S. (2004). *Salmonella* redirects phagosomal maturation. Curr. Opin. Microbiol. **7:** 78–84.

Bucci, C., Thomsen, P., Nicoziani, P., McCarthy, J., and van Deurs, B. (2000). Rab7: A key to lysosome biogenesis. Mol. Biol. Cell **11:** 467–480.

Carter, C., Pan, S., Zouhar, J., Avila, E.L., Girke, T., and Raikhel, N.V. (2004). The vegetative vacuole proteome of *Arabidopsis thaliana* reveals predicted and unexpected proteins. Plant Cell **16:** 3285–3303.

Catalano, C.M., Czymmek, K.J., Gann, J.G., and Sherrier, D.J. (2007). *Medicago truncatula* syntaxin SYP132 defines the symbiosome membrane and infection droplet membrane in root nodules. Planta **225:** 541–550.

Cheon, C.-I., Lee, N.-G., Siddique, A.-B.M., Bal, A.K., and Verma, D.P.S. (1993). Roles of plant homologs of Rab1p and Rab7p in the biogenesis of the peribacteroid membrane, a subcellular compartment formed de novo during root nodule symbiosis. EMBO J. **12:** 4125–4135.

Chow., C.M., Neto, H., Foucart, C., and Moore, I. (2008). Rab-A2 and Rab-A3 GTPases define a trans-golgi endosomal membrane domain in Arabidopsis that contributes substantially to the cell plate. Plant Cell **20:** 101–123.

Clemens, D.L., Lee, B.Y., and Horwitz, M.A. (2000a). *Mycobacterium tuberculosis* and *Legionella pneumophila* phagosomes exhibit arrested maturation despite acquisition of Rab7. Infect. Immun. **68:** 5154–5166.

Clemens, D.L., Lee, B.Y., and Horwitz, M.A. (2000b). Deviant expression of Rab5 on phagosomes containing the intracellular pathogens *Mycobacterium tuberculosis* and *Legionella pneumophila* is associated with altered phagosomal fate. Infect. Immun. **68:** 2671–2684.

Conrad, P.A., Smart, E.J., Ying, Y.S., Anderson, R.G., and Bloom, G.S. (1995). Caveolin cycles between plasma membrane caveolae and the Golgi complex by microtubule-dependent and microtubule-independent steps. J. Cell Biol. **131:** 1421–1433.

Dettmer, J., Hong-Hermesdorf, A., Stierhof, Y.-D., and Schumacher, K. (2006). Vacuolar H^+-ATPase activity is required for endocytic and secretory trafficking in *Arabidopsis.* Plant Cell **18:** 715–730.

Ebine, K., Okatani, Y., Uemura, T., Goh, T., Shoda, K., Niihama, M., Terao Morita, M., Spitzer, C., Otegui, M.S., Nakano, A., and Ueda, T. (2008). A SNARE complex unique to seed plants is required for protein storage vacuole biogenesis and seed development of *Arabidopsis thaliana.* Plant Cell **20:** 3006–3021.

Ebine, K., and Ueda, T. (2009). Unique mechanism of plant endocytic/vacuolar transport pathways. J. Plant Res. **122:** 21–30.

Foresti, O., daSilva, L.L.P., and Denecke, J. (2006). Overexpression of the *Arabidopsis* syntaxin PEP12/SYP21 inhibits transport from the prevacuolar compartment to the lytic vacuole *in vivo.* Plant Cell **18:** 2275–2293.

Geldner, N., and Jürgens, G. (2006). Endocytosis in signalling and development. Curr. Opin. Plant Biol. **9:** 589–594.

Gerrard, S.R., Levi, B.P., and Stevens, T.H. (2000). Pep12p is a multifunctional yeast syntaxin that controls entry of biosynthetic, endocytic and retrograde traffic into the prevacuolar compartment. Traffic **1:** 259–269.

Haas, T.J., Sliwinski, M.K., Martinez, D.E., Preuss, M., Ebine, K., Ueda, T., Nielsen, E., Odorizzi, G., and Oteguia, M.S. (2007). The *Arabidopsis* AAA ATPase SKD1 is involved in multivesicular endosome function and interacts with its positive regulator LYST-INTERACTING PROTEIN5. Plant Cell **19:** 1295–1312.

Harrison, R.E., Brumell, J.H., Khandani, A., Bucci, C., Scott, C.C., Jiang, X., Finlay, B.B., and Grinstein, S. (2004). Salmonella impairs RILP recruitment to Rab7 during maturation of invasion vacuoles. Mol. Biol. Cell **15:** 3146–3154.

Jaillais, Y., Fobis-Loisy, I., Miège, C., and Gaude, T. (2008). Evidence for a sorting endosome in Arabidopsis root cells. Plant J. **53:** 237–247.

Jauh, G.Y., Phillips, T.E., and Rogers, J.C. (1999). Tonoplast intrinsic protein isoforms as markers for vacuolar functions. Plant Cell **11:** 1867–1882.

Jones, K.M., Kobayashi, H., Davies, B.W., Taga, M.E., and Walker, G.C. (2007). How rhizobial symbionts invade plants: The *Sinorhizobium*-Medicago model. Nat. Rev. Microbiol. **5:** 619–633.

Jürgens, G. (2004). Membrane trafficking in plants. Annu. Rev. Cell Dev. Biol. **20:** 481–504.

Karimi, M., Inze, D., and Depicker, A. (2002). GATEWAY vectors for *Agrobacterium*-mediated plant transformation. Trends Plant Sci. **7:** 193–195.

Knodler, L.A., Celli, J., and Finlay, B.B. (2001). Pathogenesis trickery: Deception of host cell processes. Nat. Rev. Mol. Cell Biol. **2:** 578–588.

Kotzer, A.M., Brandizzi, F., Neumann, U., Paris, N., Moore, I., and Hawes, C. (2004). AtRabF2b (Ara7) acts on the vacuolar trafficking pathway in tobacco leaf epidermal cells. J. Cell Sci. **117:** 6377–6389.

Lam, S.K., Siu, C.L., Hillmer, S., Jang, S., An, G., Robinson, D.G., and Jiang, L. (2007a). Rice SCAMP1 defines clathrin-coated, trans-golgi-located tubular-vesicular structures as an early endosome in tobacco BY-2 cells. Plant Cell **19:** 296–319.

Lam, S.K., Tse, Y.C., Robinson, D.G., and Jiang, L. (2007). Tracking down the elusive early endosome. Trends Plant Sci. **12:** 497–505.

Li, Y.B., Rogers, S.W., Tse, Y.C., Lo, S.W., Sun, S.S., Jauh, G.Y., and Jiang, L. (2002). BP-80 and homologs are concentrated on post-Golgi, probable lytic prevacuolar compartments. Plant Cell Physiol. **43:** 726–742.

Limpens, E., Mirabella, R., Fedorova, E., Franken, C., Franssen, H., Bisseling, T., and Geurts, R. (2005). Formation of organelle-like

N_2-fixing symbiosomes in legume root nodules is controlled by DMI2. Proc. Natl. Acad. Sci. USA **102:** 10375–10380.

Limpens, E., Ramos, J., Franken, C., Raz, V., Compaan, B., Franssen, H., Bisseling, T., and Geurts, R. (2004). RNA interference in *Agrobacterium rhizogenes*-transformed roots of Arabidopsis and *Medicago truncatula.* J. Exp. Bot. **55:** 983–992.

Lipka, V., Kwon, C., and Panstruga, R. (2007). SNARE-Ware: The role of SNARE-domain proteins in plant biology. Annu. Rev. Cell Dev. Biol. **23:** 147–174.

Mayor, S., and Pagano, R.E. (2007). Pathways of clathrin-independent endocytosis. Nat. Rev. Mol. Cell Biol. **8:** 603–612.

Mellor, R.B. (1989). Bacteroids in the Rhizobium-legume symbiosis inhabit a plant internal lytic compartment: Implications for other microbial endosymbioses. J. Exp. Bot. **40:** 831–839.

Méresse, S., Gorvel, J.P., and Chavrier, P.J. (1995). The rab7 GTPase resides on a vesicular compartment connected to lysosomes. J. Cell Sci. **108:** 3349–3358.

Mo, B., Tse, Y.C., and Jiang, L. (2006). Plant prevacuolar/endosomal compartments. Int. Rev. Cytol. **253:** 95–129.

Nahm, M.Y., Kim, S.W., Yun, D., Lee, S.Y., Cho, M.J., and Bahk, J.D. (2003). Molecular and biochemical analyses of OsRab7, a rice Rab7 homolog. Plant Cell Physiol. **44:** 1341–1349.

Nielsen, E., Cheung, A.Y., and Ueda, T. (2008). The regulatory RAB and ARF GTPases for vesicular trafficking. Plant Physiol. **147:** 1516–1526.

Otegui, M.S., Herder, R., Schulze, J., Jung, R., and Staehelin, L.A. (2006). The proteolytic processing of seed storage proteins in *Arabidopsis* embryo cells starts in the multivesicular bodies. Plant Cell **18:** 2567–2581.

Paris, N., and Neuhaus, J.M. (2002). BP-80 as a vacuolar sorting receptor. Plant Mol. Biol. **50:** 903–914.

Passey, S., Bradley, A., and Mellor, H. (2008). *Escherichia coli* isolated from bovine mastitis invade mammary cells by a modified endocytic pathway. Vet. Microbiol. **130:** 151–164.

Pelham, H.R. (2002). Insights from yeast endosomes. Curr. Opin. Cell Biol. **14:** 454–462.

Perret, E., Lakkaraju, A., Deborde, S., Schreiner, R., and Rodriguez-Boulan, E. (2005). Evolving endosomes: how many varieties and why? Curr. Opin. Cell Biol. **17:** 423–434.

Pfeffer, S., and Aivazian, D. (2004). Targeting Rab GTPases to distinct membrane compartments. Nat. Rev. Mol. Cell Biol. **5:** 886–896.

Pfeffer, S.R. (2007). Unsolved mysteries in membrane traffic. Annu. Rev. Biochem. **76:** 629–645.

Rink, J., Ghigo, E., Kalaidzidis, Y., and Zerial, M. (2005). Rab conversion as a mechanism of progression from early to late endosomes. Cell **122:** 735–749.

Robert, S., Chary, S.N., Drakakaki, G., Li, S., Yang, Z., Raikhel, N.V., and Hicks, G.R. (2008). Endosidin1 defines a compartment involved in endocytosis of the brassinosteroid receptor BRI1 and the auxin transporters PIN2 and AUX1. Proc. Natl. Acad. Sci. USA **105:** 8464–8469.

Robinson, D.G., Jiang, L., and Schumacher, K. (2008). The endosomal system of plants: Charting new and familiar territories. Plant Physiol. **147:** 1482–1492.

Rojo, E., Zouhar, J., Kovaleva, V., Hong, S., and Raikhel, N.V. (2003). The AtC-VPS protein complex is localized to the tonoplast and the prevacuolar compartment in Arabidopsis. Mol. Biol. Cell **14:** 361–369.

Roth, L.E., and Stacey, G. (1989). Bacterium release into host cells of nitrogen-fixing soybean nodules: The symbiosome membrane comes from three sources. Eur. J. Cell Biol. **49:** 13–23.

Rutherford, S., and Moore, I. (2002). The Arabidopsis Rab GTPase family: Another enigma variation. Curr. Opin. Plant Biol. **5:** 518–528.

Saito, C., Ueda, T., Abe, H., Wada, Y., Kuroiwa, T., Hisada, A., Furuya, M., and Nakano, A.A. (2002). Complex and mobile structure form a distinct subregion within the continuous vacuolar membrane in young cotyledons of Arabidopsis. Plant J. **29:** 245–255.

Samaj, J., Read, N.D., Volkmann, D., Menzel, D., and Baluska, F. (2005). The endocytic network in plants. Trends Cell Biol. **15:** 424–433.

Sanderfoot, A. (2007). Increases in the number of SNARE genes parallels the rise of multicellularity among the green plants. Plant Physiol. **144:** 6–17.

Sanderfoot, A., Kovaleva, V., Zheng, H., and Raikhel, N. (1999). The t-SNARE AtVAM3p resides on the prevacuolar compartment in Arabidopsis root cells. Plant Physiol. **121:** 929–938.

Sanderfoot, A.A., Assaad, F.F., and Raikhel, N.V. (2000). The Arabidopsis genome. An abundance of soluble N-ethylmaleimide-sensitive factor adaptor protein receptors. Plant Physiol. **124:** 1558–1569.

Sanderfoot, A.A., Kovaleva, V., Bassham, D.C., and Raikhel, N.V. (2001). Interactions between syntaxins identify at least five SNARE complexes within the Golgi/prevacuolar system of the Arabidopsis cell. Mol. Biol. Cell **12:** 3733–3743.

Sato, M.H., Nakamura, N., Ohsumi, Y., Kouchi, H., Kondo, M., Hara-Nishimura, I., Nishimura, M., and Wada, Y. (1997). The AtVAM3 encodes a syntaxin-related molecule implicated in the vacuolar assembly in *Arabidopsis thaliana*. J. Biol. Chem. **272:** 24530–24535.

Sanmartín, M., Ordóñez, A., Sohn, E.J., Robert, S., Sánchez-Serrano, J.J., Surpin, M.A., Raikhel, N.V., and Rojo, E. (2007). Divergent functions of VTI12 and VTI11 in trafficking to storage and lytic vacuoles in Arabidopsis. Proc. Natl. Acad. Sci. USA **104:** 3645–3650.

Schimmöller, F., and Riezman, H. (1993). Involvement of Ypt7p, a small GTPase, in traffic from late endosome to the vacuole in yeast. J. Cell Sci. **106:** 823–830.

Seabra, M.C., and Wasmeier, C. (2004). Controlling the location and activation of Rab GTPases. Curr. Opin. Cell Biol. **16:** 451–457.

Shin, J.S., and Abraham, S.N. (2001). Co-option of endocytic functions of cellular caveolae by pathogens. Immunology **102:** 2–7.

Shin, J.S., Gao, Z., and Abraham, S.N. (2000). Involvement of cellular caveolae in bacterial entry into mast cells. Science **289:** 785–788.

Smit, P., Raedts, J., Portyanko, V., Debellé, F., Gough, C., Bisseling, T., and Geurts, R. (2005). NSP1 of the GRAS protein family is essential for rhizobial Nod factor-induced transcription. Science **308:** 1789–1791.

Sohn, E.J., Kim, E.S., Zhao, M., Kim, S.J., Kim, H., Kim, Y.-W., Lee, Y.J., Hillmer, S., Sohn, U., Jiang, L., and Hwang, I. (2003). Rha1, an *Arabidopsis* Rab5 homolog, plays a critical role in the vacuolar trafficking of soluble cargo proteins. Plant Cell **15:** 1057–1070.

Son, O., et al. (2003). Expression of *srab7* and *SCaM* genes required for endocytosis of *Rhizobium* in root nodules. Plant Sci. **165:** 1239–1244.

Sonti, R.V., Chiurazzi, M., Wong, D., Davies, C.S., Harlow, G.R., Mount, D.W., and Signer, E.R. (1995). Arabidopsis mutants deficient in T-DNA integration. Proc. Natl. Acad. Sci. USA **92:** 11786–11790.

Surpin, M., and Raikhel, N. (2004). Traffic jams affect plant development and signal transduction. Nat. Rev. Mol. Cell Biol. **5:** 100–109.

Surpin, M., Zheng, H., Morita, M.T., Saito, C., Avila, E., Blakeslee, J.J., Bandyopadhyay, A., Kovaleva, V., Carter, D., Murphy, A., Tasaka, M., and Raikhel, N. (2003). The VTI family of SNARE proteins is necessary for plant viability and mediates different protein transport pathways. Plant Cell **15:** 2885–2899.

Tamura, K., Dudley, J., Nei, M., and Kumar, S. (2007). MEGA4: Molecular Evolutionary Genetics Analysis (MEGA) software version 4.0. Mol. Biol. Evol. **24:** 1596–1599.

Thijssen, M.H., Mittempergher, F., Van Aelst, A.C., and Van Went, J.L. (1997). Improved ultrastructural preservation of Petunia and Brassica ovules and embryo sacs by high pressure freesing and freeze substitution. Protoplasma **197:** 199–209.

Tse, Y.C., Mo, B., Hillmer, S., Zhao, M., Lo, S.W., Robinson, D.G., and Jianga, L. (2004). Identification of multivesicular bodies as prevacuolar compartments in *Nicotiana tabacum* BY-2 cells. Plant Cell **16:** 672–693.

Ueda, T., Uemura, T., Sato, M.H., and Nakano, A. (2004). Functional differentiation of endosomes in *Arabidopsis* cells. Plant J. **40:** 783–789.

Ueda, T., Yamaguchi, M., Uchimiyia, H., and Nakano, A. (2001). Ara6, a plant unique novel type Rab GTPase, functions in the endocytic pathway of *Arabidopsis thaliana.* EMBO J. **17:** 4730–4741.

Uemura, T., Ueda, T., Ohniwa, R.L., Nakano, A., Takeyasu, K., and Sato, M.H. (2004). Systematic analysis of SNARE molecules in Arabidopsis: Dissection of the post-Golgi network in plant cells. Cell Struct. Funct. **29:** 49–65.

Uemura, T., Yoshimura, S.H., Takeyasu, K., and Sato, M.H. (2002). Vacuolar membrane dynamics revealed by GFP–AtVam3 fusion protein. Genes Cells **7:** 743–753.

Van de Velde, W., Pérez Guerra, J.C., De Keyser, A., De Rycke, R., Rombauts, S., Maunoury, N., Mergaert, P., Kondorosi, E., Holsters, M., and Goormachtig, S. (2006). Aging in legume symbiosis. A molecular view on nodule senescence in *Medicago truncatula.* Plant Physiol. **141:** 711–720.

Vasse, J., de Billy, F., Camut, S., and Truchet, G. (1990). Correlation between ultrastructural differentiation of bacteroids and nitrogen fixation in alfalfa nodules. J. Bacteriol. **172:** 4295–4306.

Via, L.E., Deretic, D., Ulmer, R.J., Hibler, N.S., Huber, L.A., and Deretic, V. (1997). Arrest of mycobacterial phagosome maturation is caused by a block in vesicle fusion between stages controlled by rab5 and rab7. J. Biol. Chem. **272:** 13326–13331.

Vieira, O.V., Botelho, R.J., and Grinstein, S. (2002). Phagosome maturation: Aging gracefully. Biochem. J. **366:** 689–704.

Vieira, O.V., Bucci, C., Harrison, R.E., Trimble, W.S., Lanzetti, L., Gruenberg, J., Schreiber, A.D., Stahl, P.D., and Grinstein, S. (2003). Modulation of Rab5 and Rab7 recruitment to phagosomes by phosphatidylinositol 3-kinase. Mol. Cell. Biol. **23:** 2501–2514.

Vincent, J.L., and Brewin, N.J. (2000). Immunolocalization of a cysteine protease in vacuoles, vesicles, and symbiosomes of pea nodule cells. Plant Physiol. **123:** 521–530.

Vonderheit, A., and Helenius, A. (2005). Rab7 associates with early endosomes to mediate sorting and transport of Semliki forest virus to late endosomes. PLoS Biol. **3:** e233.

Wang, J., Li, Y., Lo, S.W., Hillmer, S., Sun, S.S., Robinson, D.G., and Jiang, L. (2007). Protein mobilization in germinating mung bean seeds involves vacuolar sorting receptors and multivesicular bodies. Plant Physiol. **143:** 1628–1639.

Wienkoop, S., and Saalbach, G. (2003). Proteome analysis. Novel proteins identified at the peribacteroid membrane from *Lotus japonicus* root nodules. Plant Physiol. **131:** 1080–1090.

Yano, D., Sato, M., Saito, C., Sato, M.H., Morita, M.T., and Tasaka, M. (2003). A SNARE complex containing SGR3/AtVAM3 and ZIG/VTI11 in gravity-sensing cells is important for Arabidopsis shoot gravitropism. Proc. Natl. Acad. Sci. USA **100:** 8589–8594.